National Science Foundation
WHERE DISCOVERIES BEGIN

Support from the NSF Tectonics Program

Pressure Solution and Fluid Flow in the Seismogenic Zone: Application to Cascadia

[1]Donald M. Fisher, [2]Greg Hirth, [3]John Hooker, [1]Andrew Smye, [6]Tsai-Wei Chen, [4]Yoshi Hashimoto, [5]Asuka Yamaguchi, Gabrielle Ramirez, Leah Youngquist

[1]Penn State University [2]Brown University [3]University of the Incarnate Word, [4]Kochi University [5]University of Tokyo [6]University of Washington

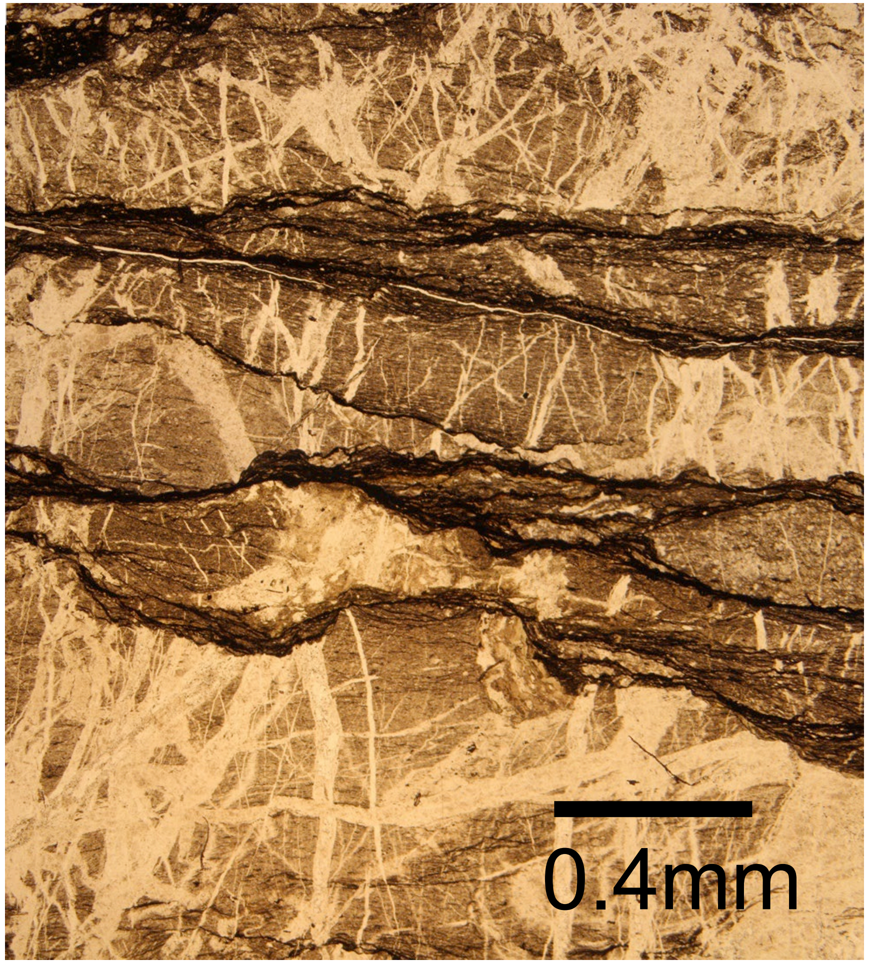

The underthrusting sediment pile

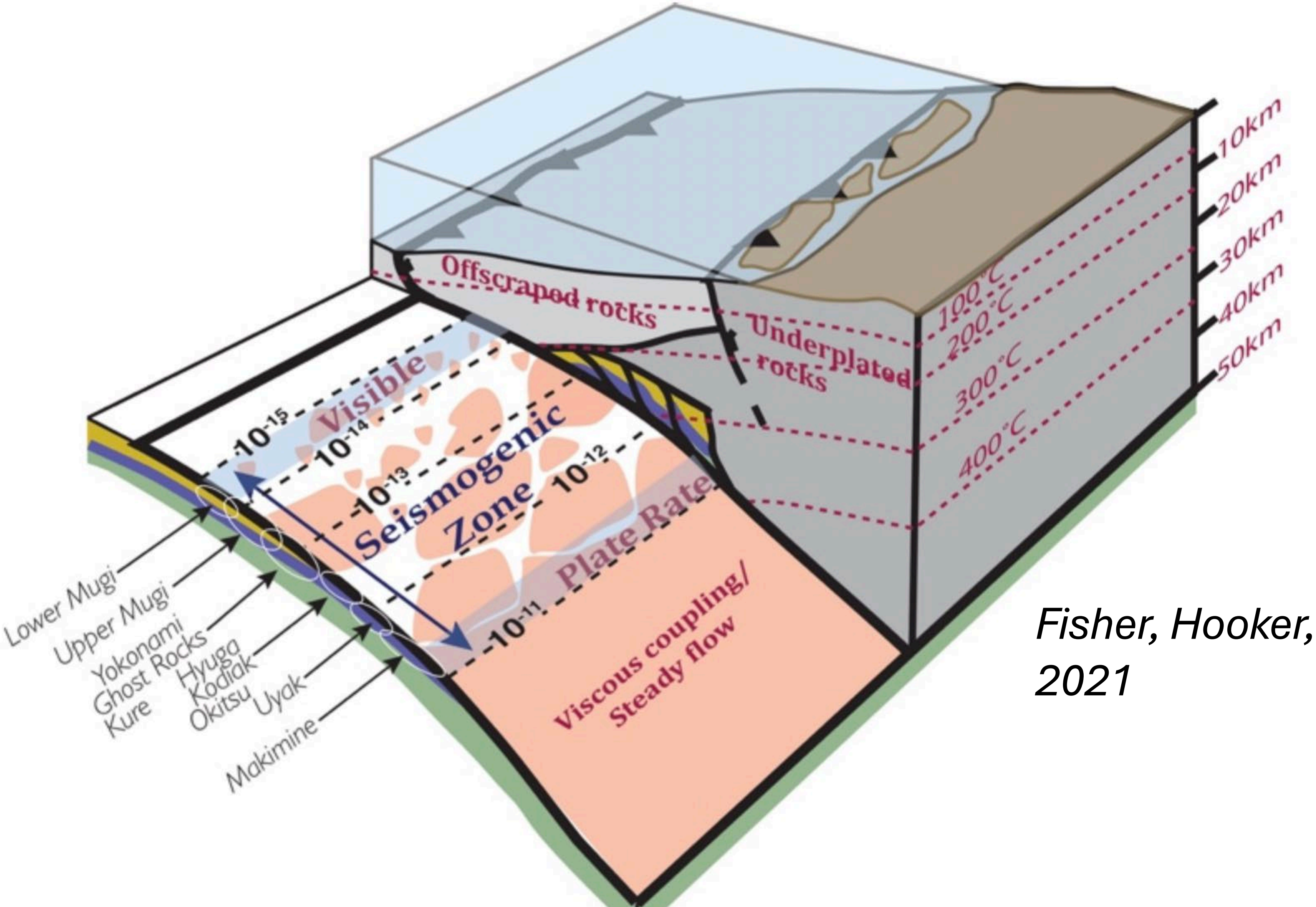

Fisher, Hooker, Smye, and Chen, 2021

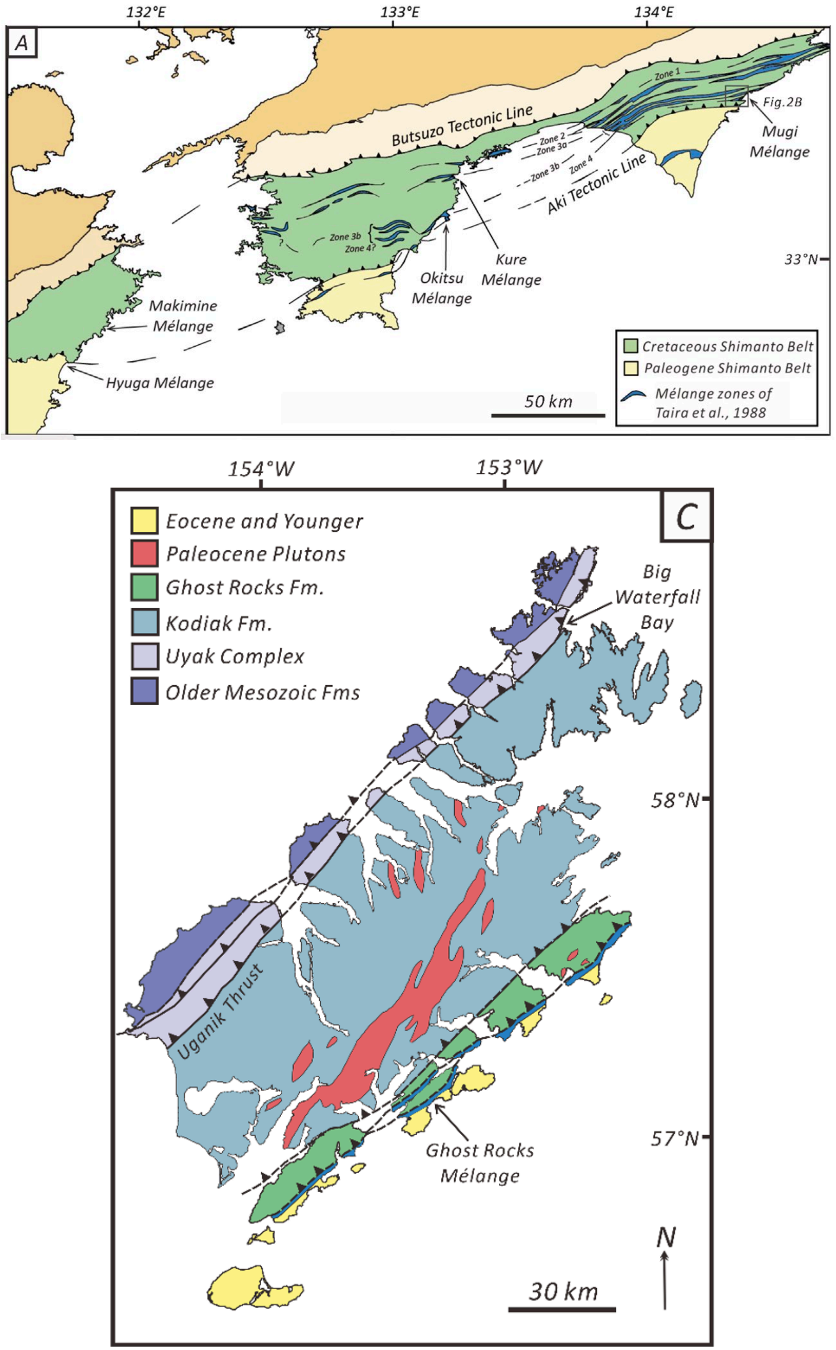

The subduction Interface

- Lie within a long-lived forearc
- Composed of oceanic crustal lithologies
- Extend along the margin for 100's of kilometers
- Lie at major boundaries between accreted packages
- Contain kinematic indicators of noncoaxial strain consistent with subduction
- Follow a compactive strain path during deformation
- Deform prior to imbrication and incorporation into the forearc wedge.

Paleotemperatures-RSCM, VR, FI, IC

Chen, Ph. D. dissertation

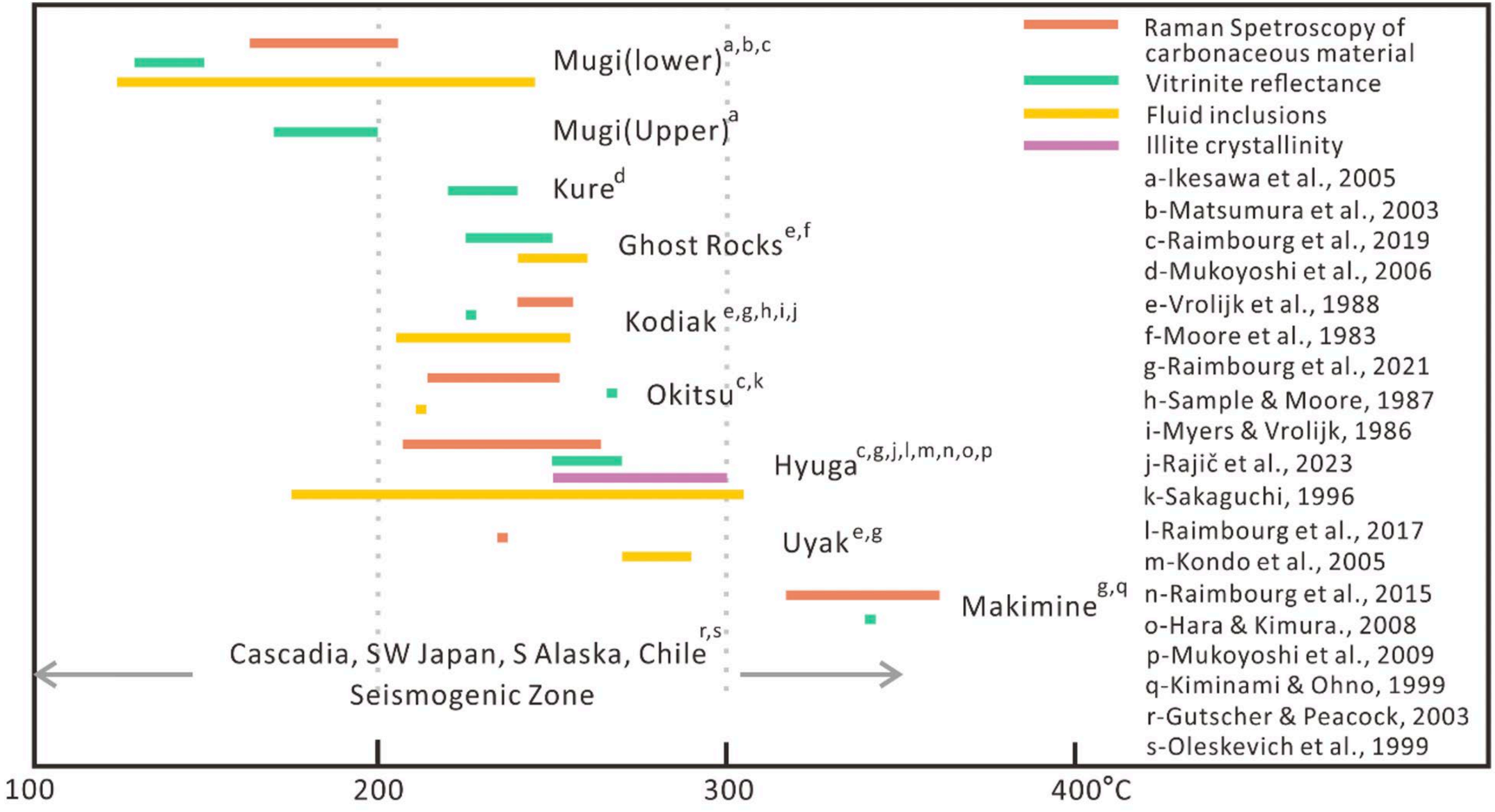

XRD

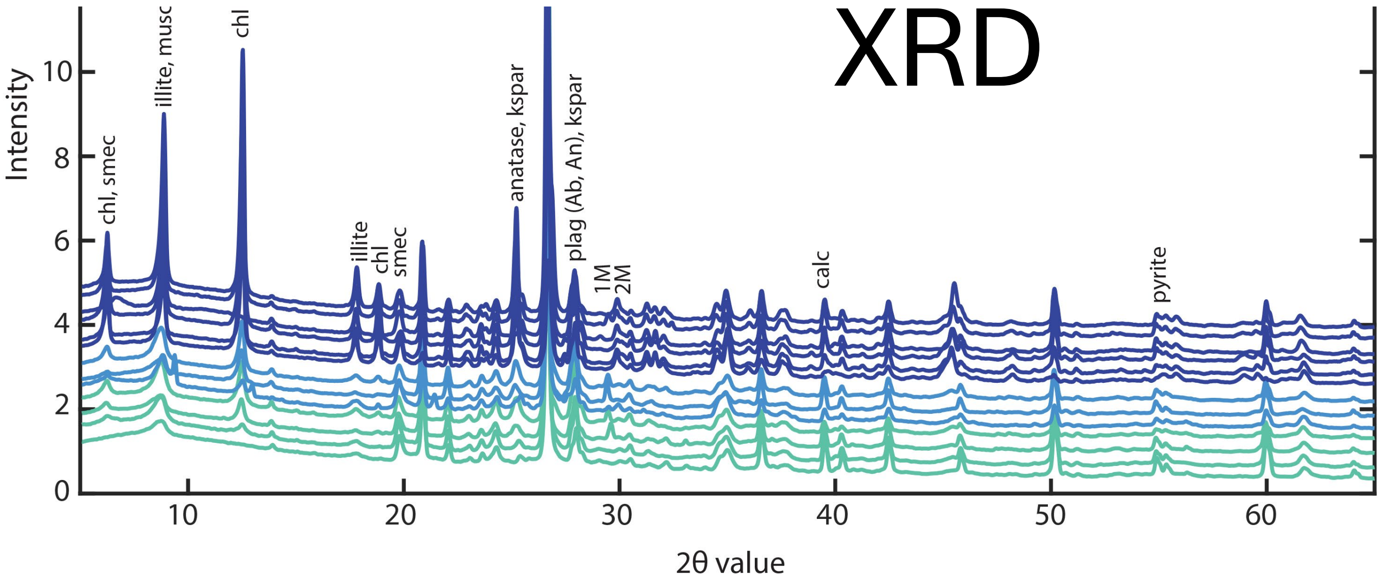

Ramirez, Smye, Fisher, Hashimoto, and Yamaguchi, 2021

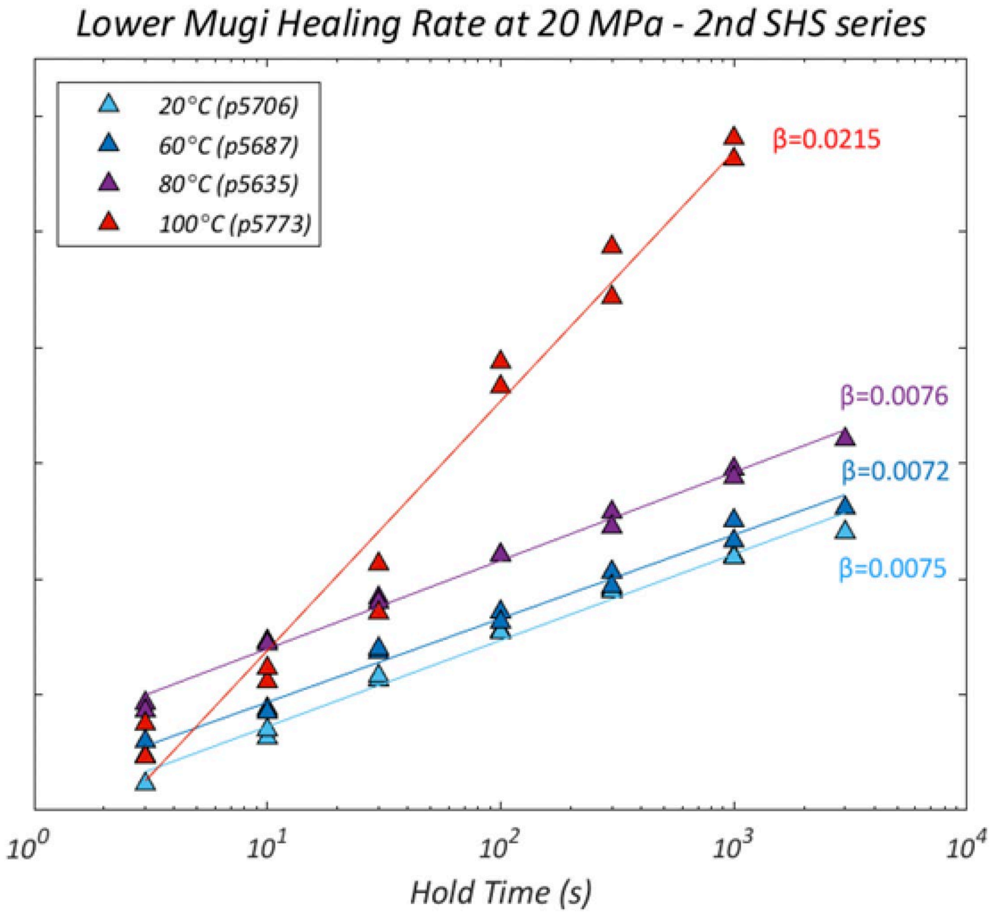

Chen, Affinito, Marone, and Fisher, 2024

Slide-Hold-Slide

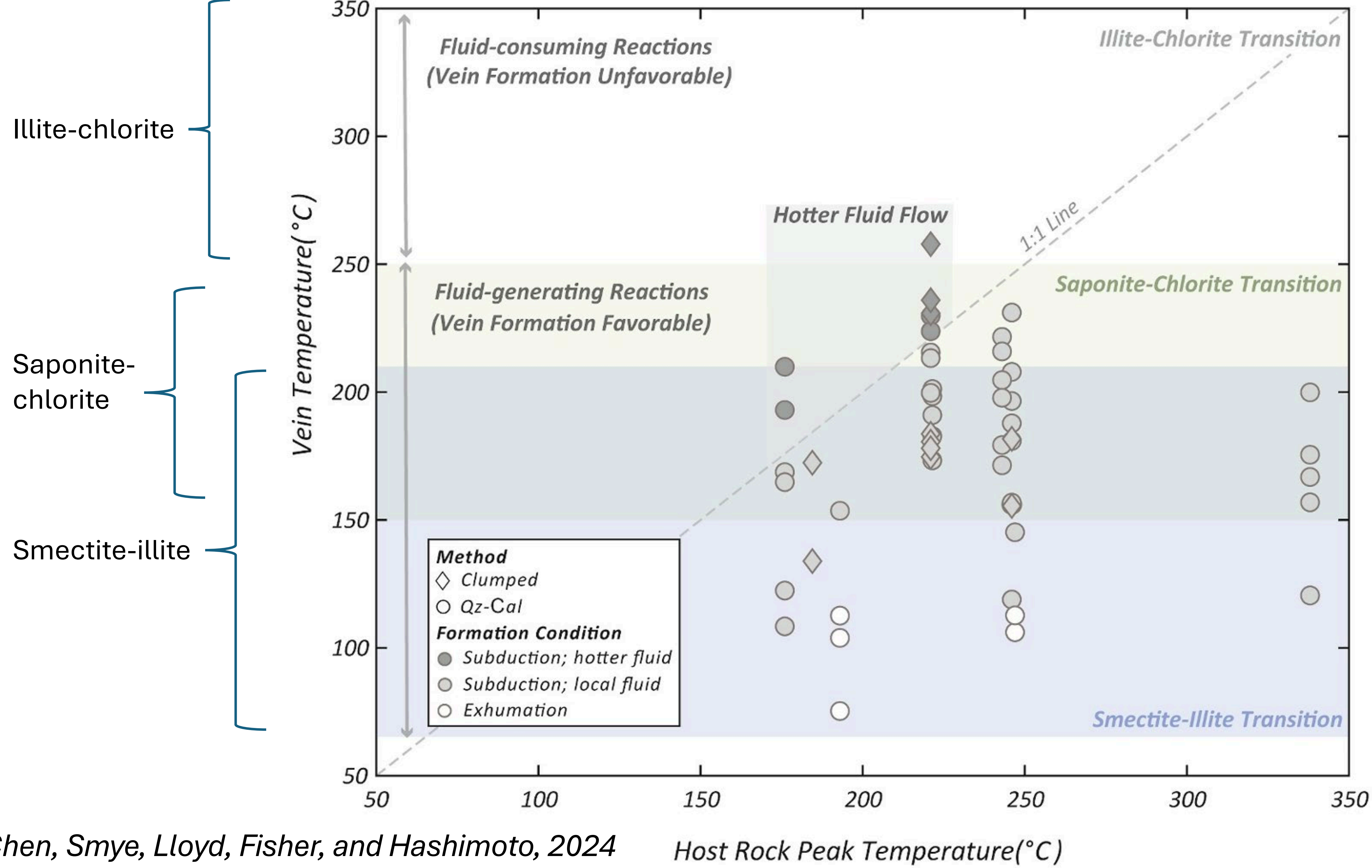

Chen, Smye, Lloyd, Fisher, and Hashimoto, 2024

Mugi lower section

Upper Mugi

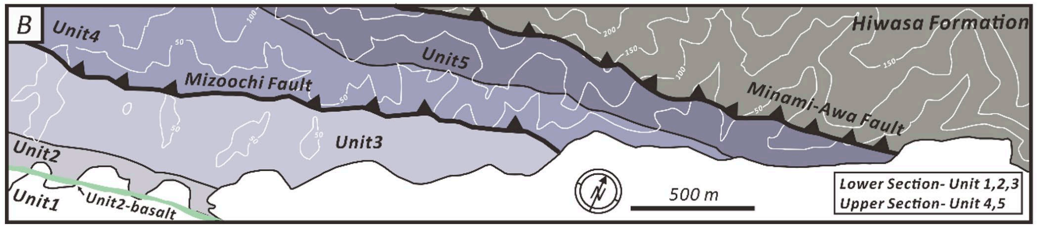
B
Unit4
Unit5
Hiwasa Formation
Mizoochi Fault
Minami-Awa Fault
Unit3
Unit2
Unit1
Unit2-basalt
500 m
Lower Section- Unit 1,2,3
Upper Section- Unit 4,5

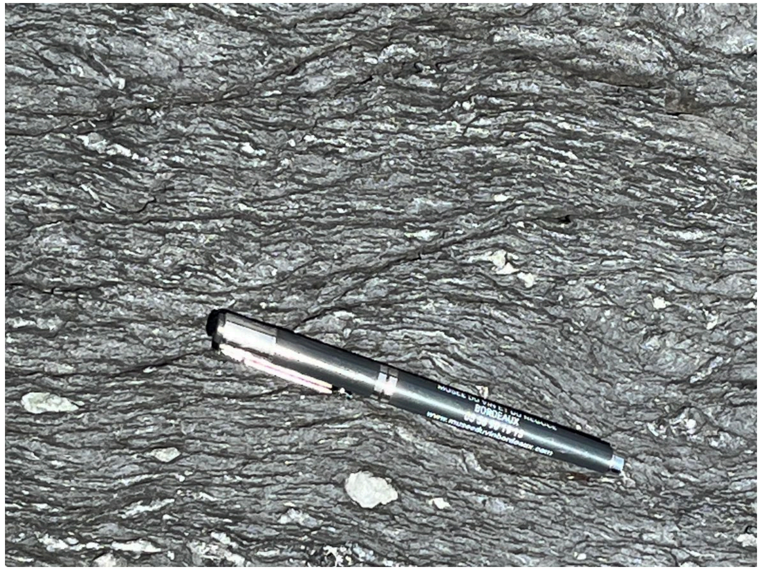

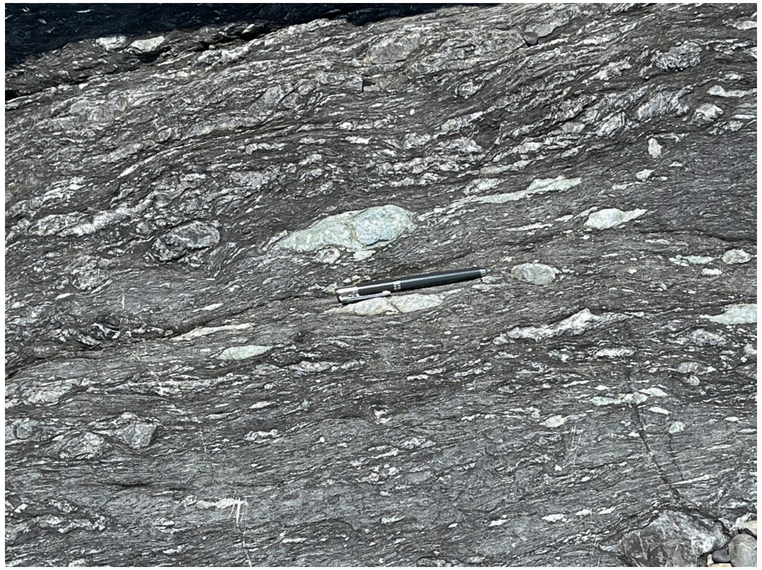

Makimine

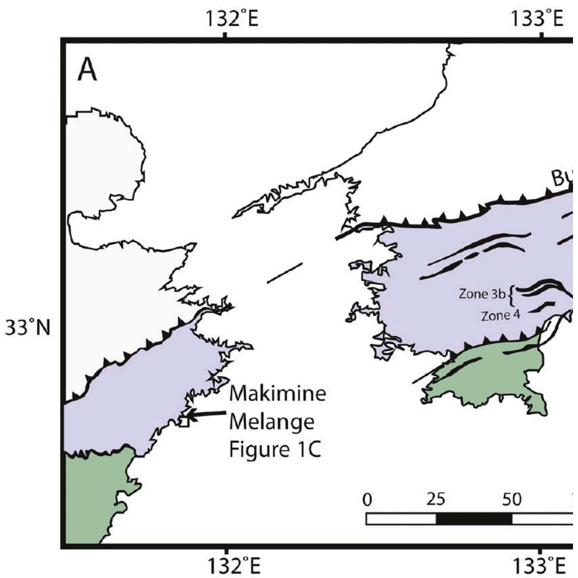
132°E
133°E
A
Zone 3b
Zone 4
33°N
Makimine
Melange
Figure 1C
0
25
50
132°E
133°E

Fisher, Hashimoto, Tonai, Tomioka, 2019*

Roof thrust

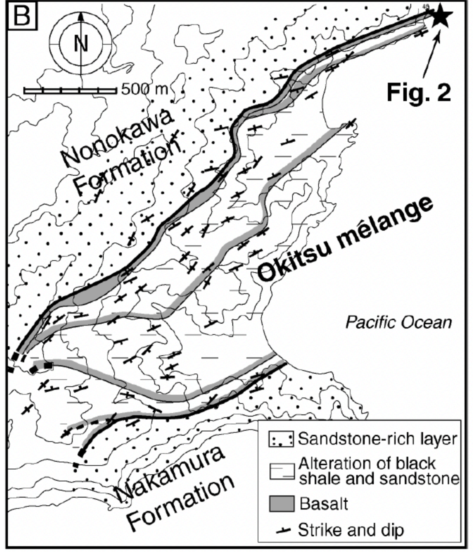

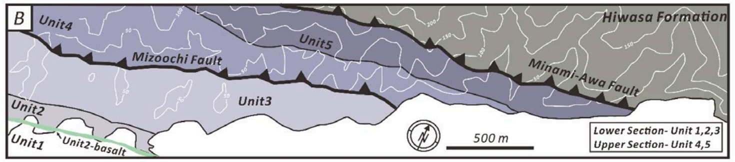

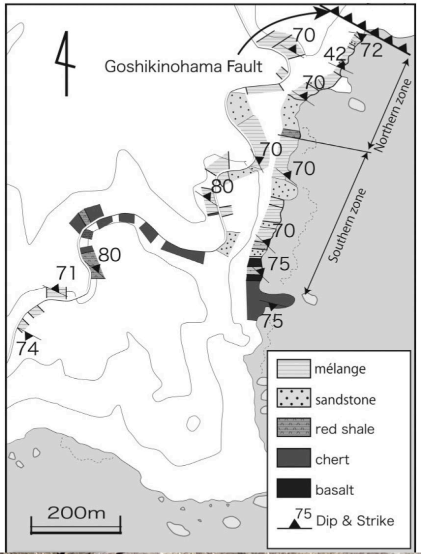

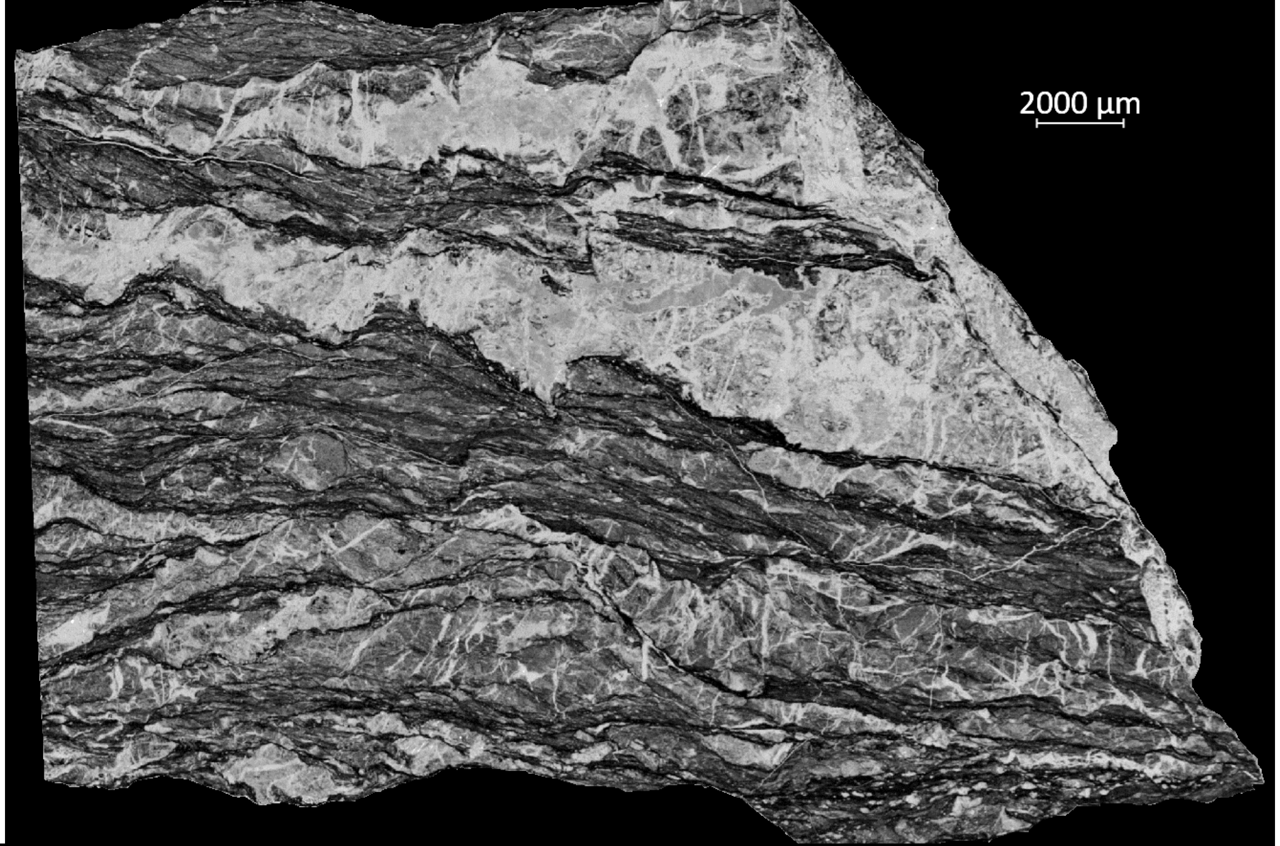
2000 µm

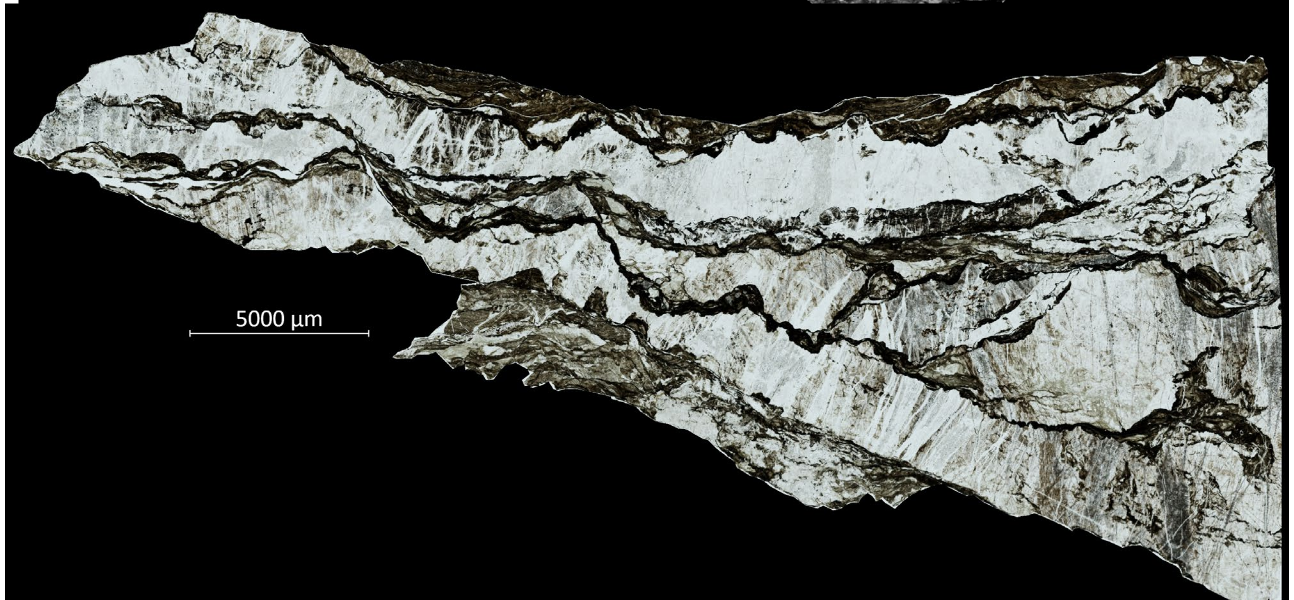
5000 µm

Veins and Scaly fabrics

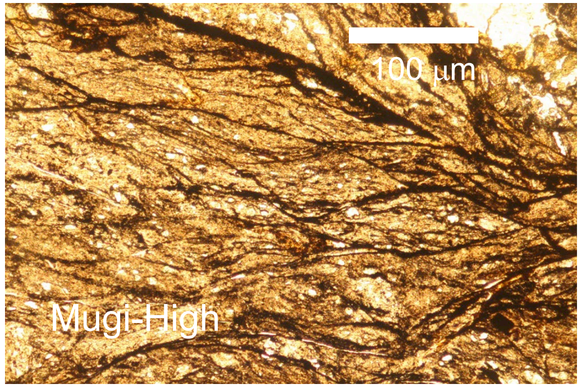

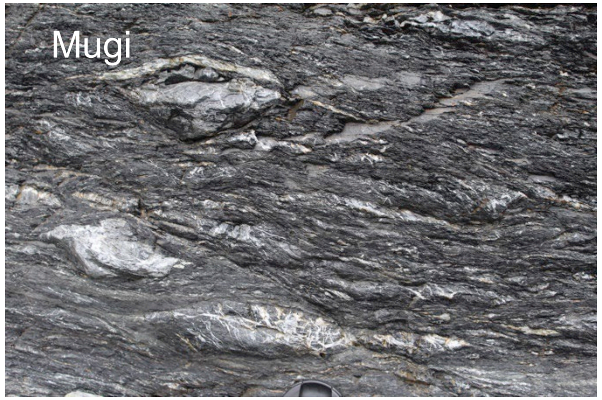

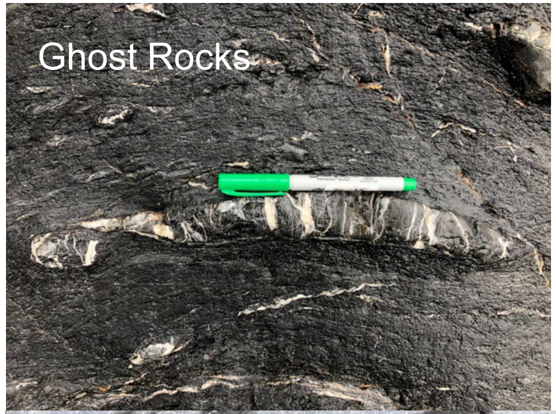

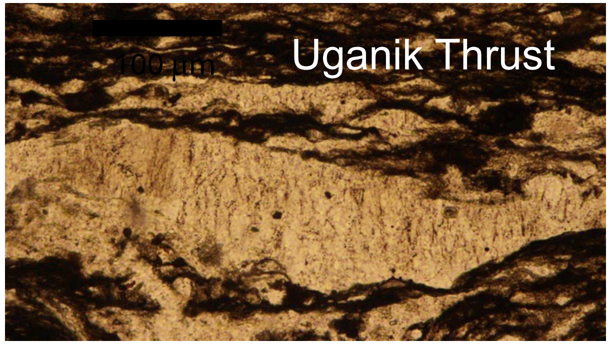

Byrne, 1984
Moore and Byrne, 1987
Fisher and Byrne, 1987
Vrolijk et al., 1988
Meneghini and Moore, 2007
Vannucchi et al., 2010
Kitamura and Kimura, 2011
Fagereng et al., 2011
Kimura et al., 2012
Yamaguchi et al., 2012
Hashimoto et al., 2012
Fisher and Brantley, 2014
Raimbourg et al., 2015
Vannucchi, 2018

Sample 9 (Upper Mugi)

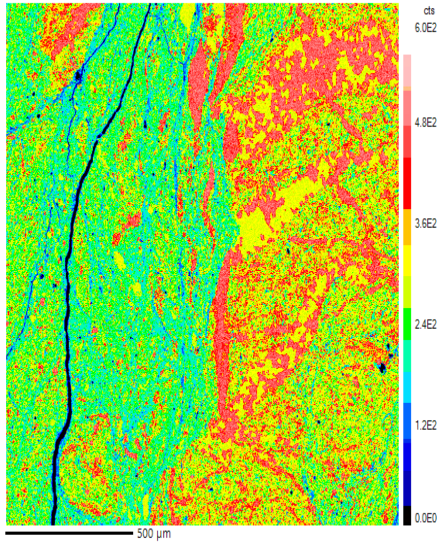

Chen, Smye, Fisher, Hashimoto, Raimbourg, and Famin, 2024a

Si removal from Scaly fabric

500 µm

AL20 (Kodiak Fm.)

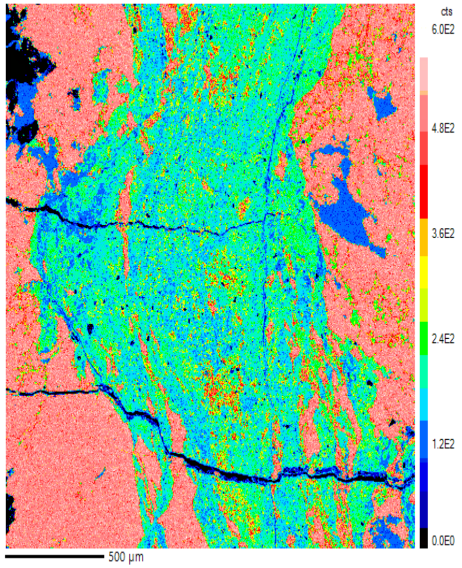

Sample 21 (Okitsu)

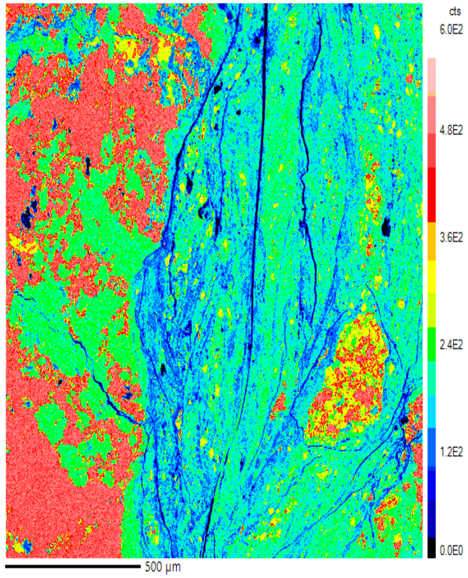

AL7-1(Uyak)

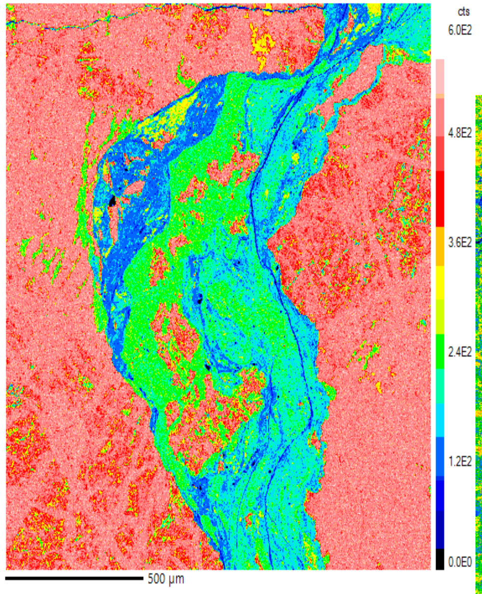

Sample 25 (Makimine)

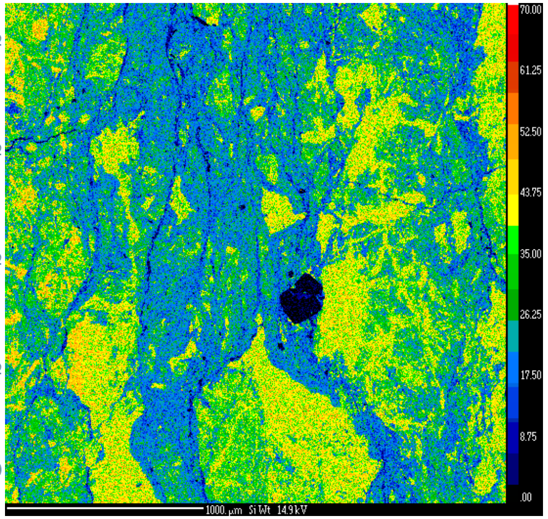

Ti enriched in the scaly fabric

Sample 9 (Upper Mugi)

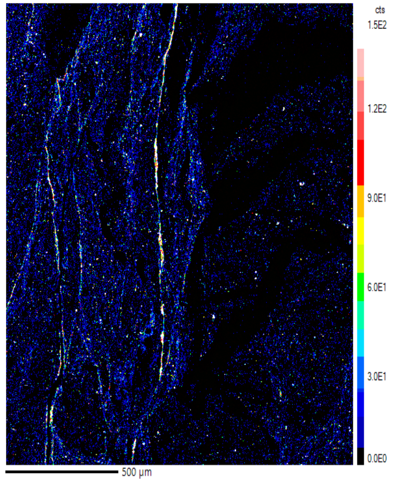

AL20 (Kodiak Fm.)

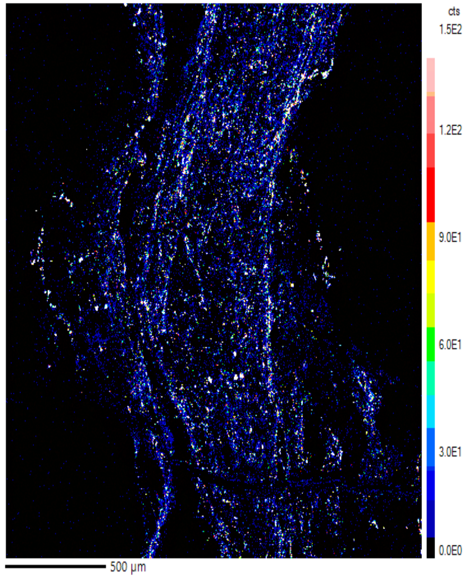

Sample 21 (Okitsu)

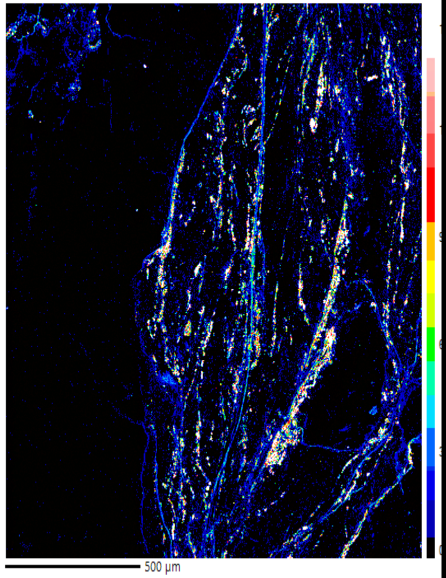

Sample 21 (Makimine)

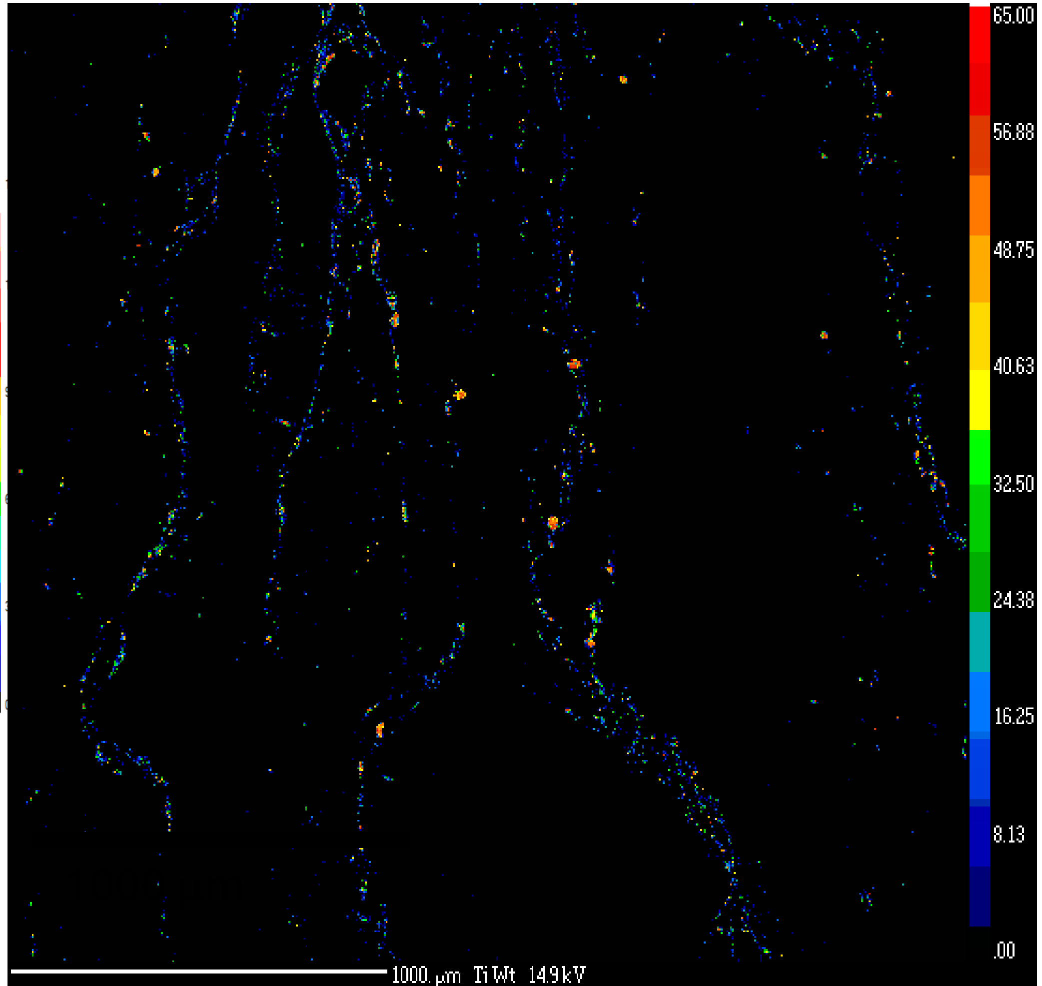

500 µm

Chen, Smye, Fisher, Hashimoto, Raimbourg, and Famin, 2024

Image Analysis

Chen, Smye, Fisher, Hashimoto, Raimbourg, and Famin, 2024

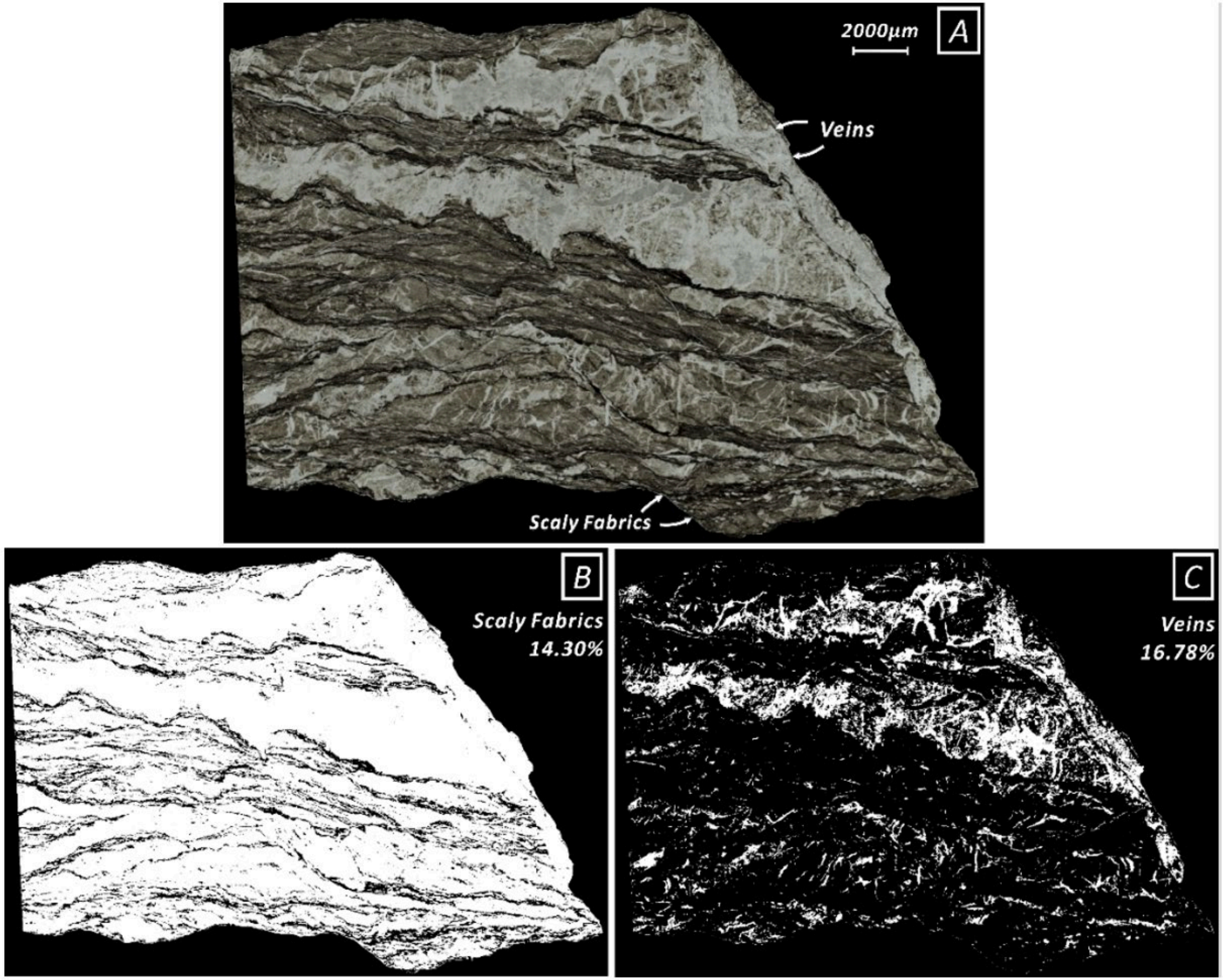

Volume strain: scaly fabric vs veins

Chen, Smye, Fisher, Hashimoto, Raimbourg, and Famin, 2024

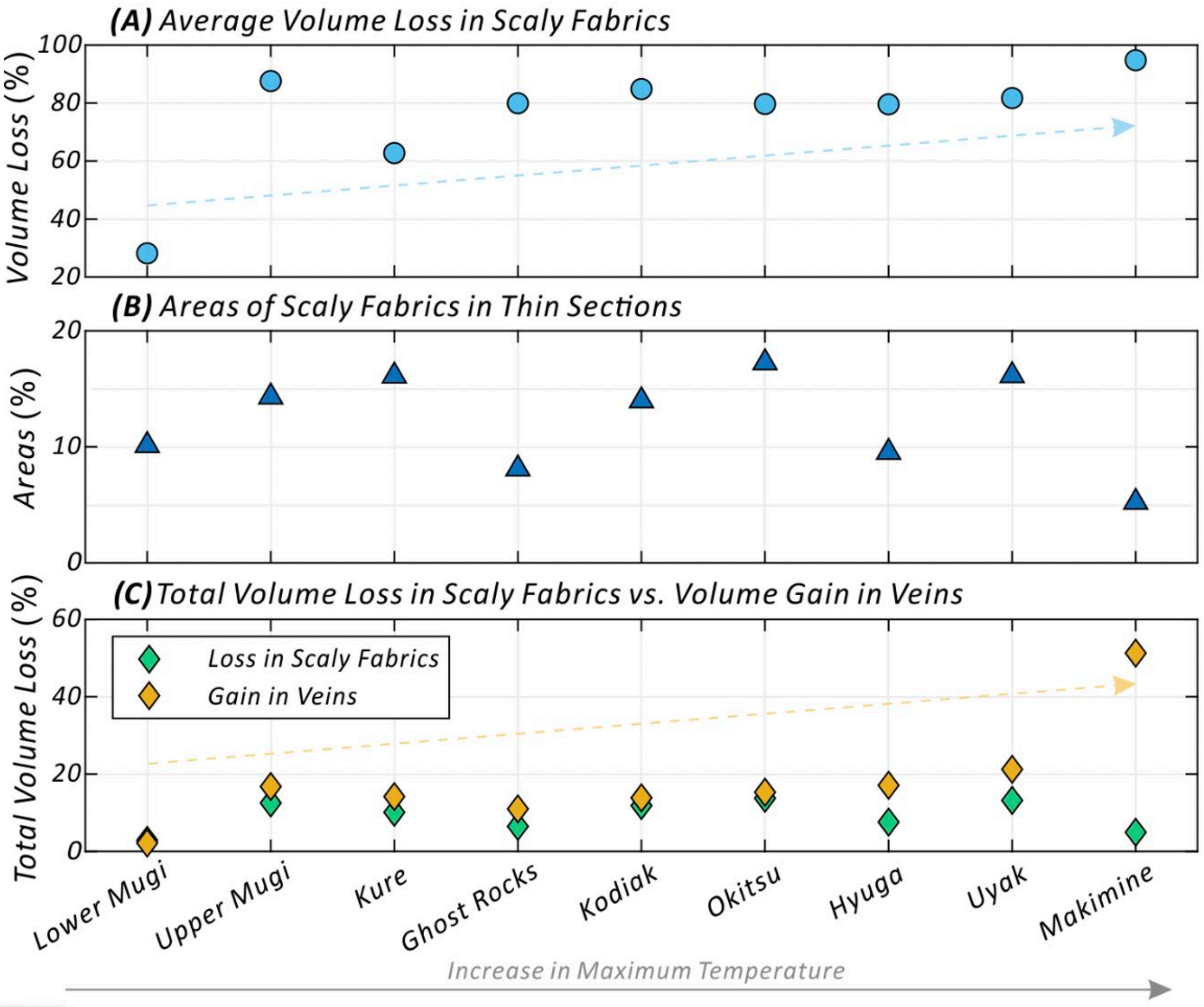

Two-stage deformation

:ory

Vertical compression

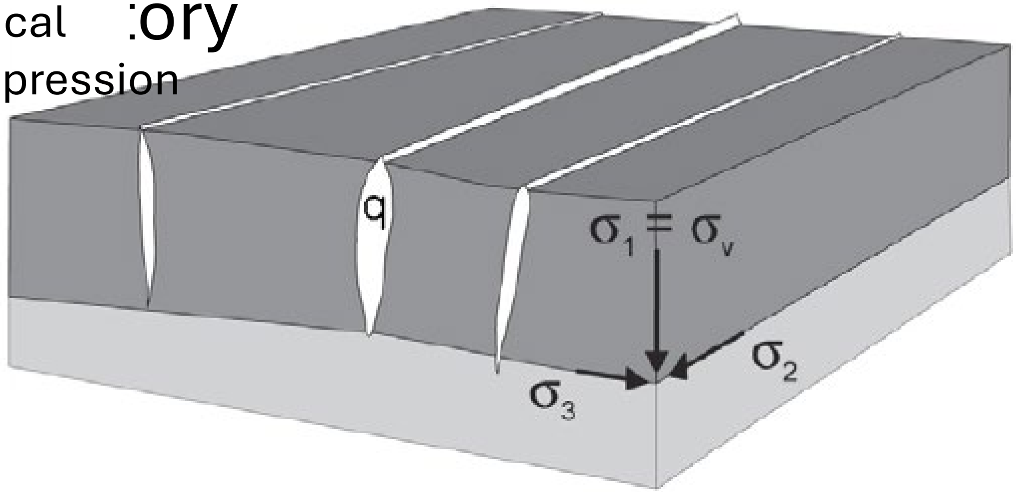

Horizontal compression

Mullions

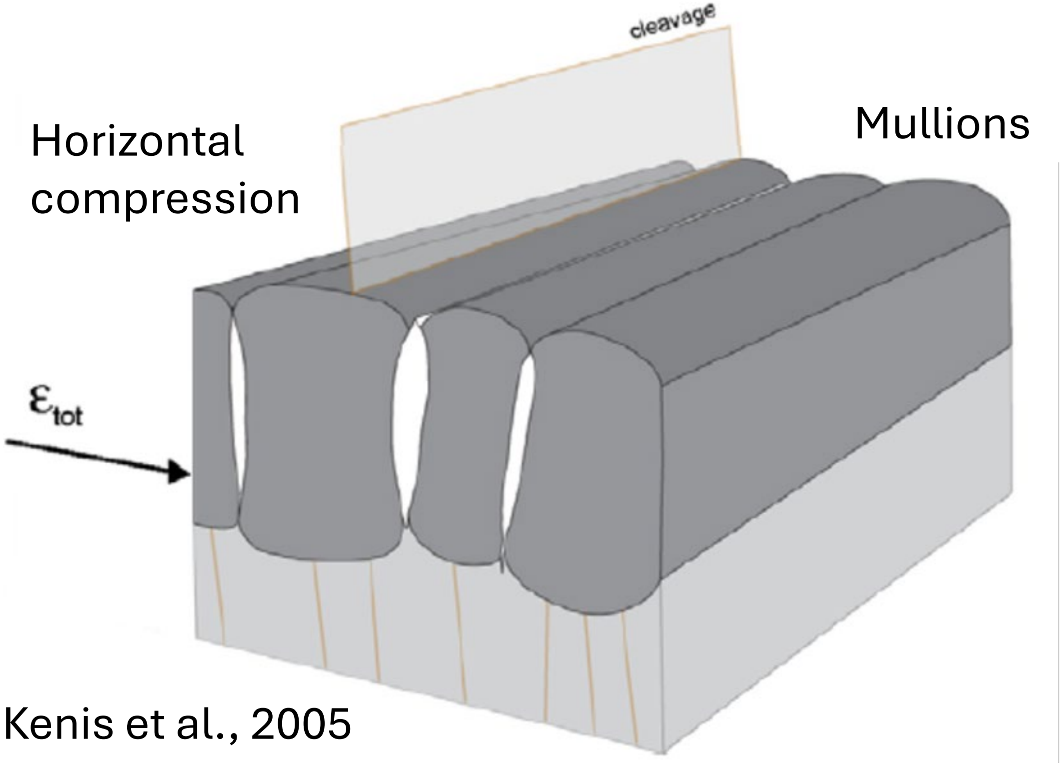

Kenis et al., 2005

Relative viscosity of vein and siliciclastic rock

Kenis Linear Viscous Flow Law

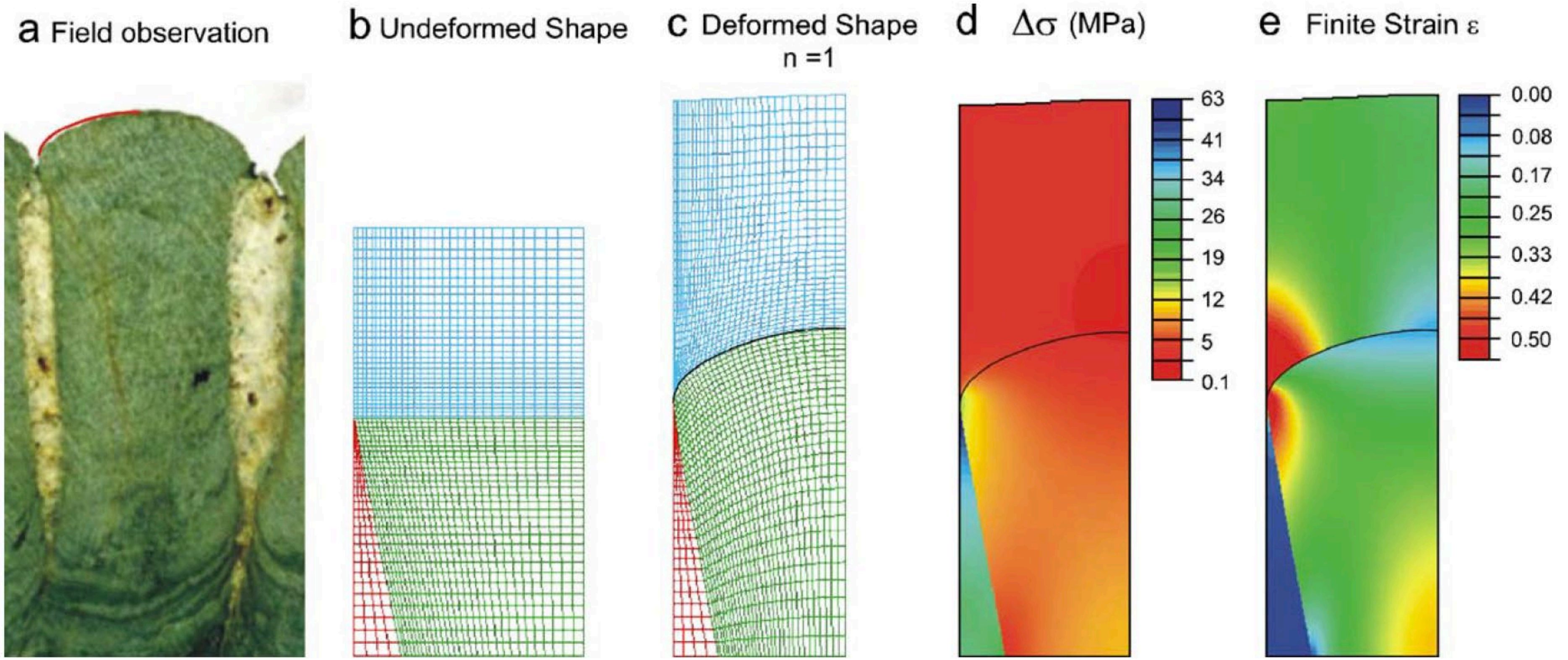

Fig. 4. Best fit solution of the case study of a mullion at Rouette (50°03′10″N–5°39′30″) showing field observation (a), undeformed (b) and deformed mesh (b) of the numerical model and contour plots of the differential stress (d) and finite strain (e) of the mullion structures. The result of the numeric solution fits well with observations of mullion shape. Stress and strain in the veins of the numerical solution are in agreement with constraints on these. Rheological properties (A_{ps}, n_{ps}) of this numeric solution are listed in Table 1 (Rouette C).

$$\dot{\varepsilon} = A'\sigma \longrightarrow \dot{\varepsilon} = AC\sigma/d^3 \exp(-Q/RT)$$

General flow law for pressure solution

$$\dot{\epsilon} = \alpha \frac{C_L D_L}{kT} \frac{w}{d^3} \bar{\sigma}.$$

C_L: concentration of mineral component in fluid (solubility)

C_L and w account for diffusion through fluid films on grain boundaries

d = grain size

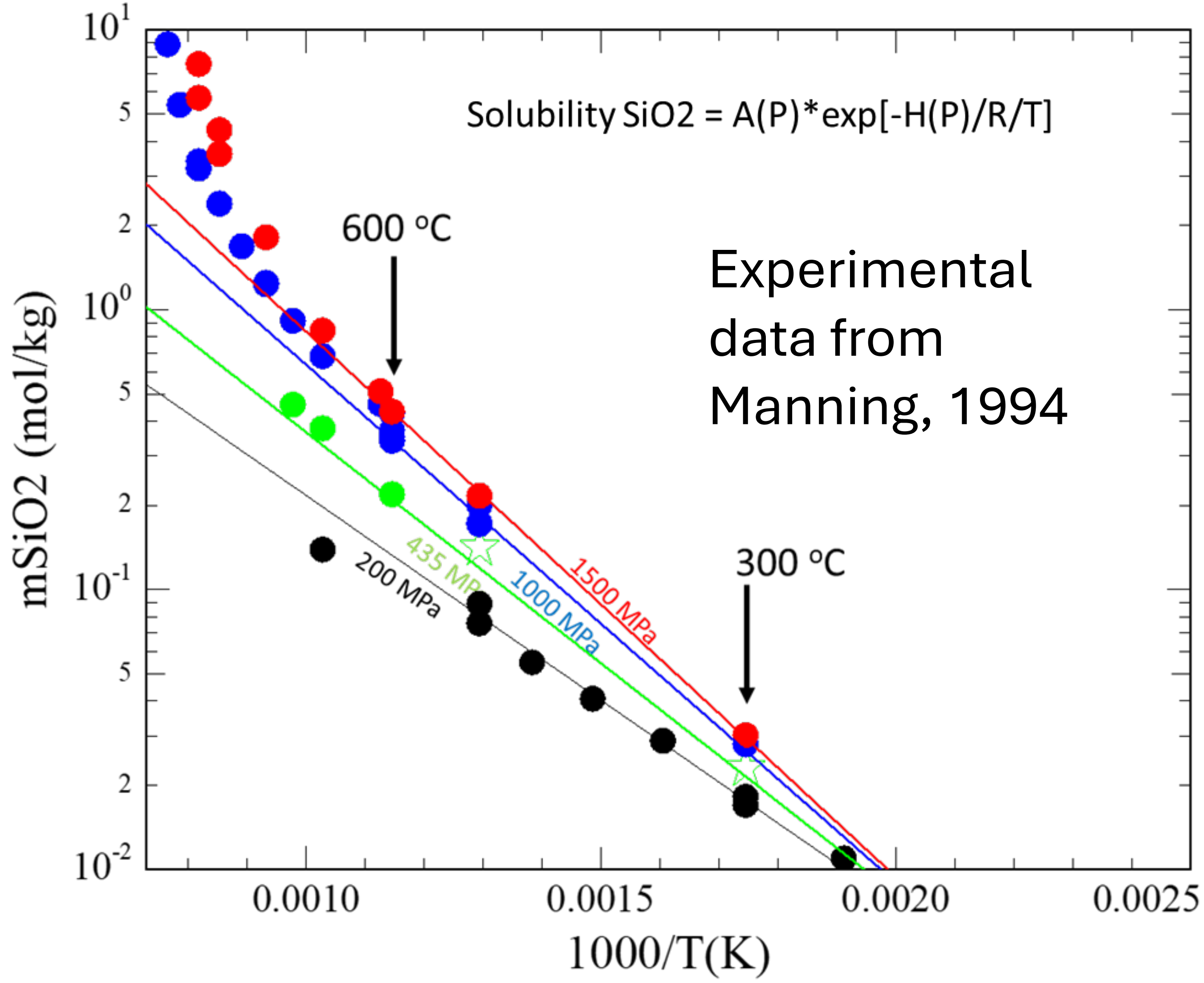

Fisher & Hirth (2024)

Kenis vs. Lab rates

Fisher and Hirth, 2024

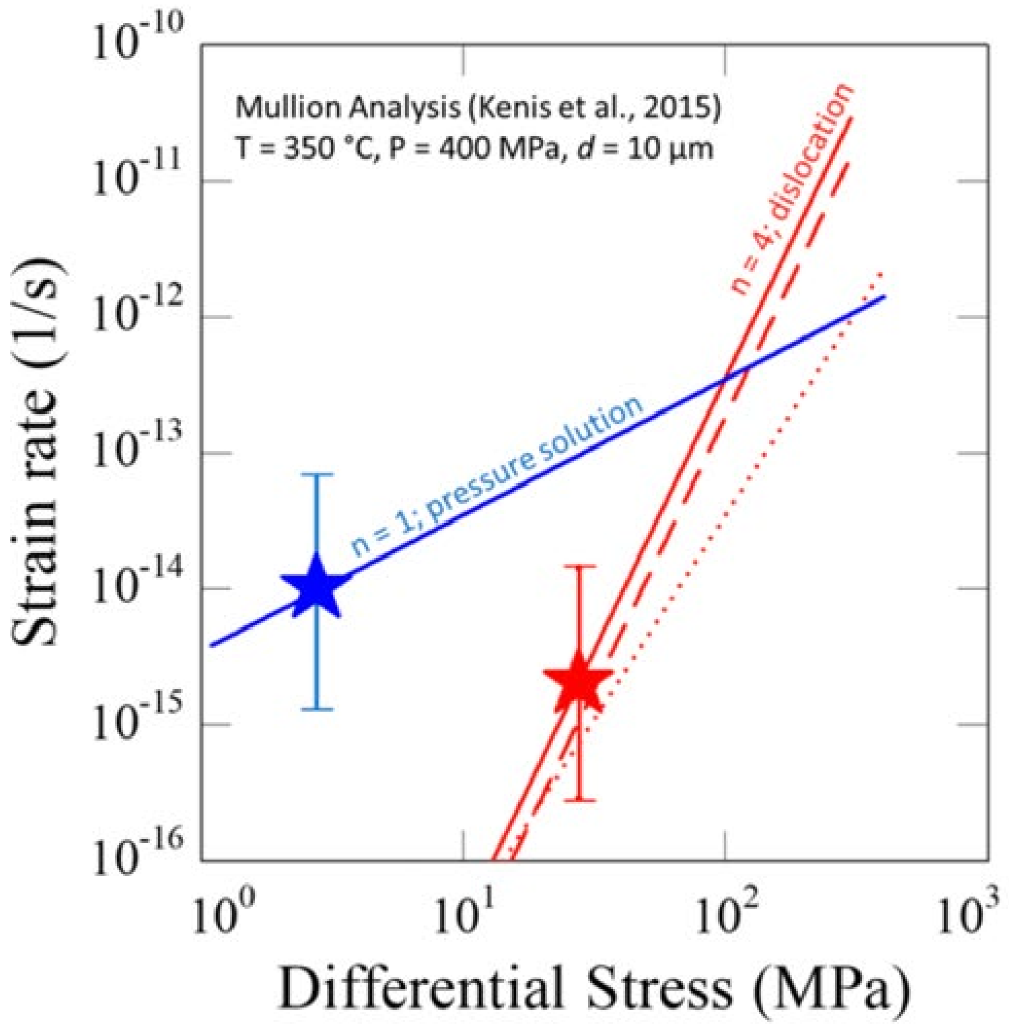

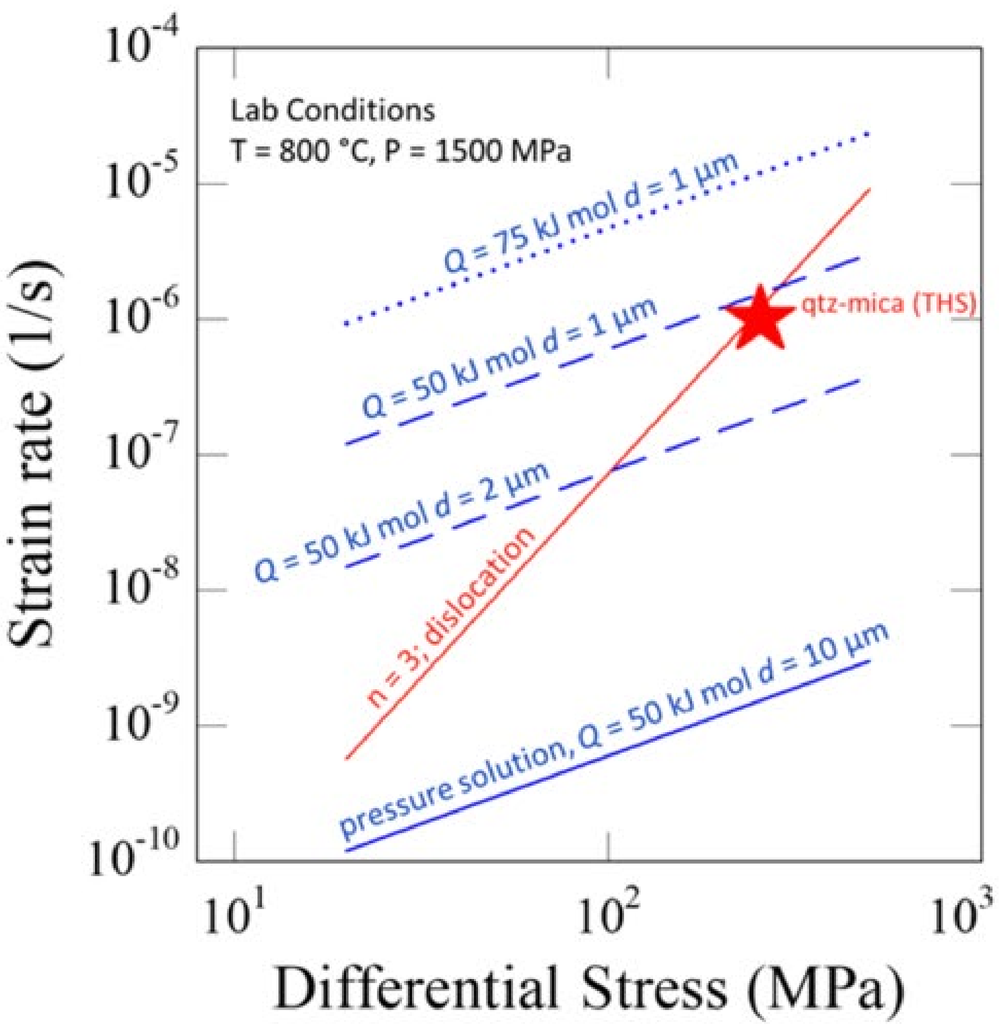

Deformation mechanisms along the Subduction Interface

Fisher and Hirth, 2024

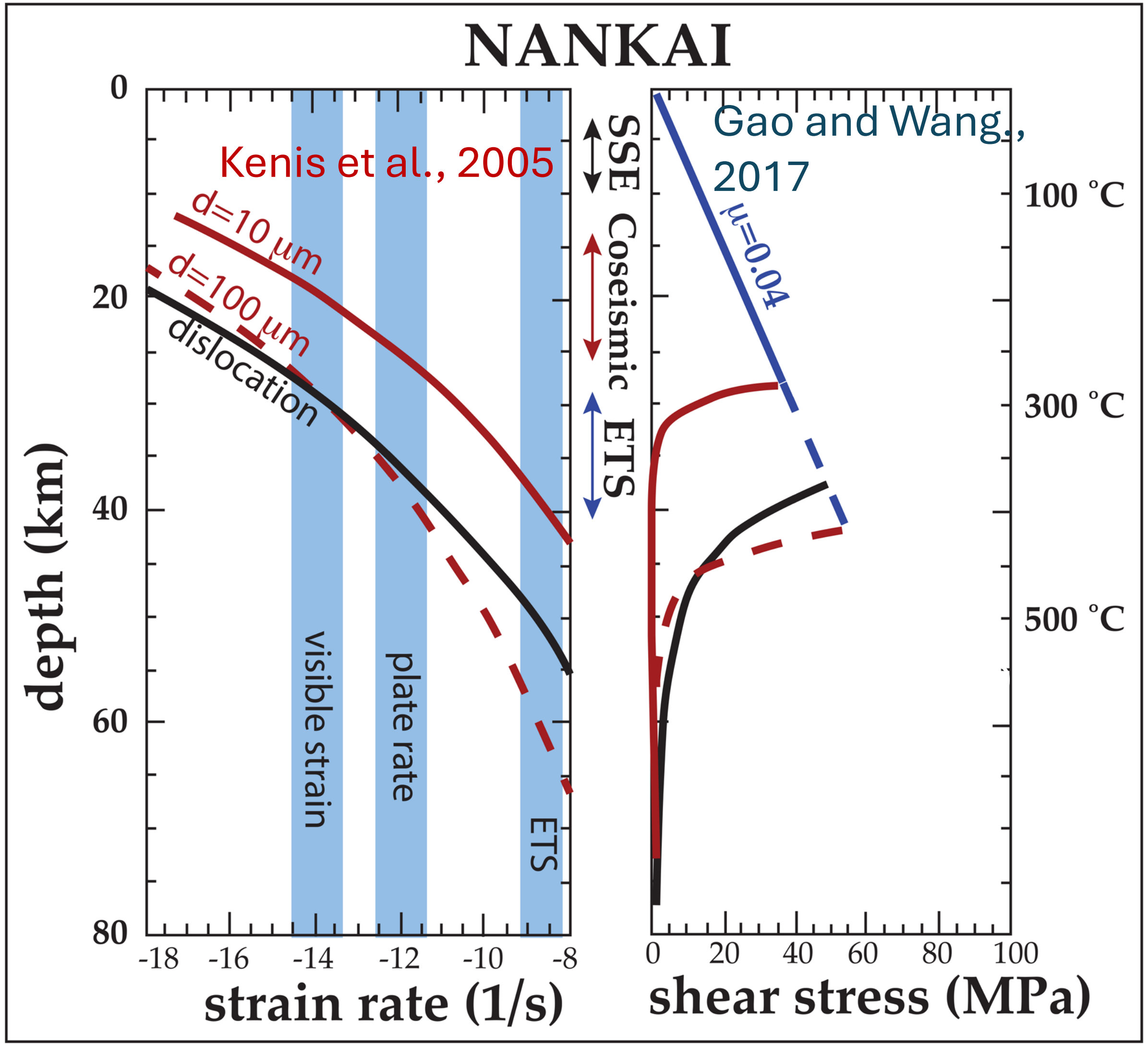

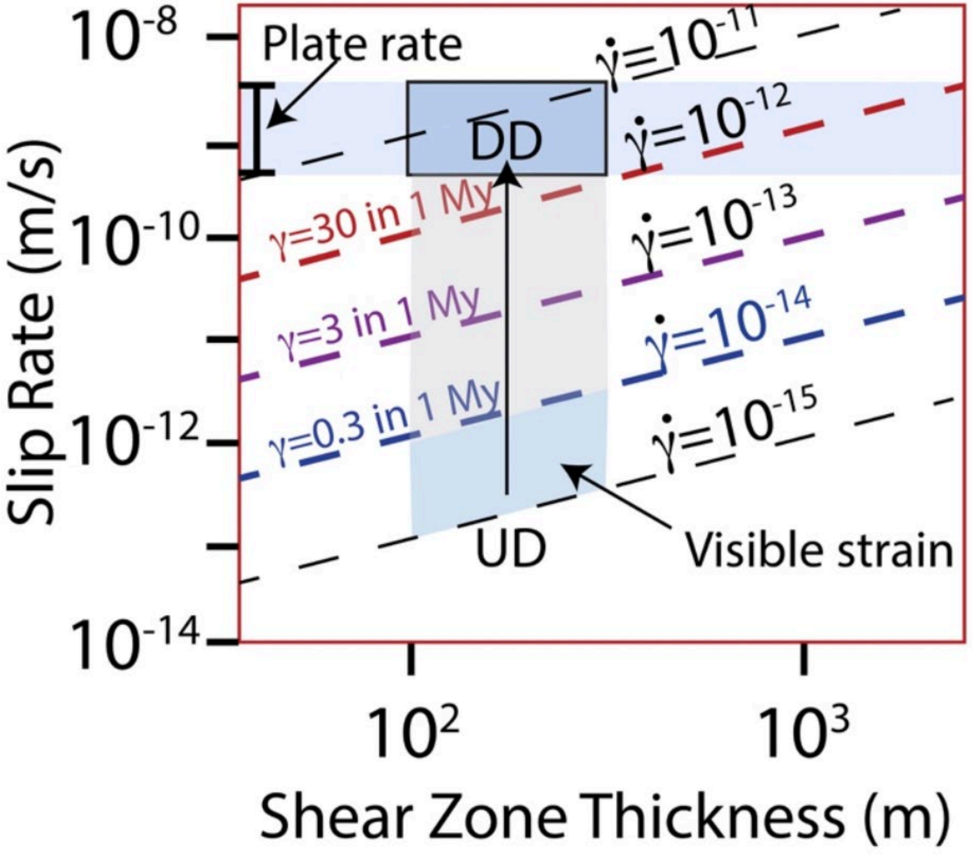

Estimates of shear zone thickness, Rowe et al., 2009

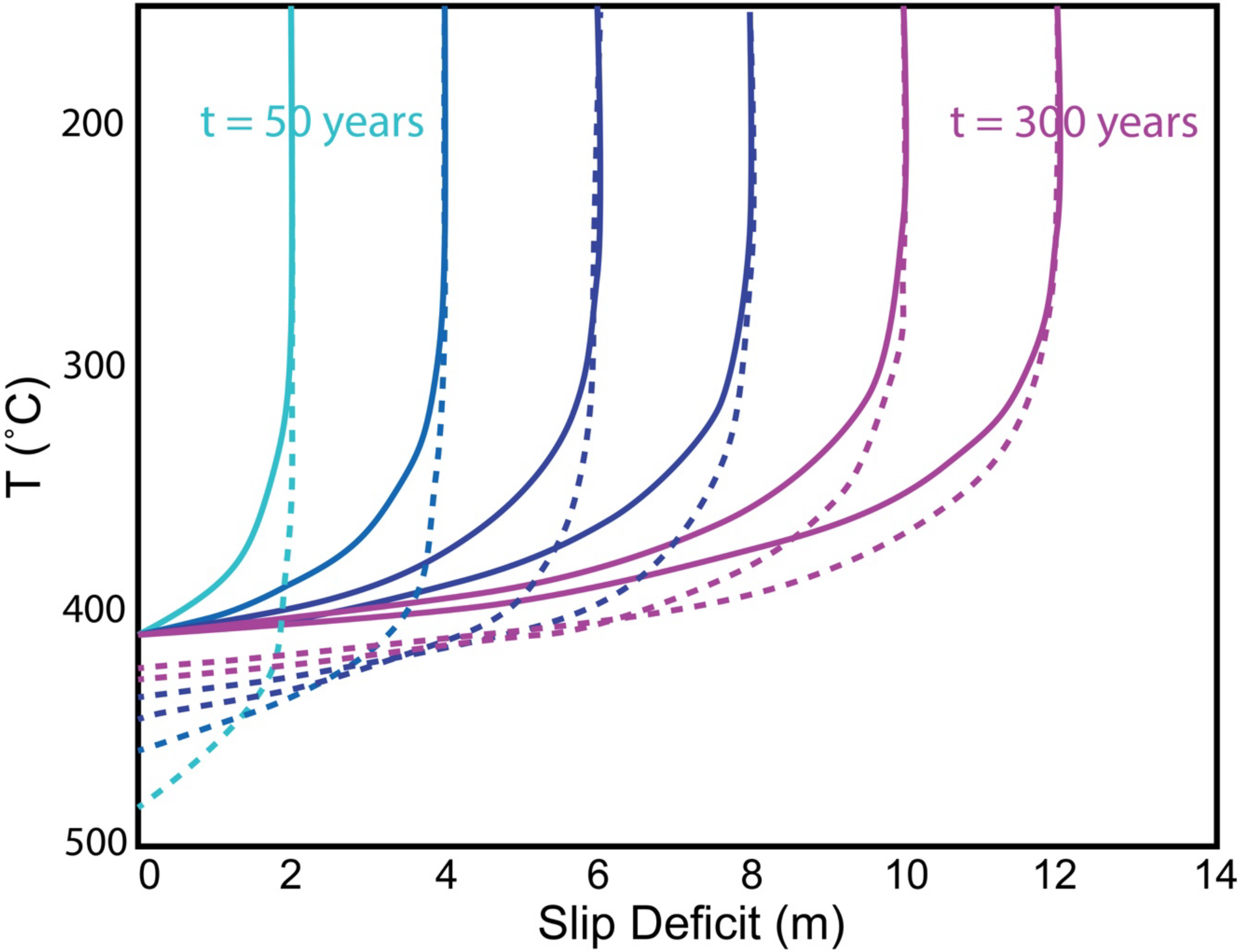

Fisher and Hirth, 2024

Inter-ETS geodetic velocity (Bartlow, 2020)

Slip-rate deficit (Melgar et al., 2022)

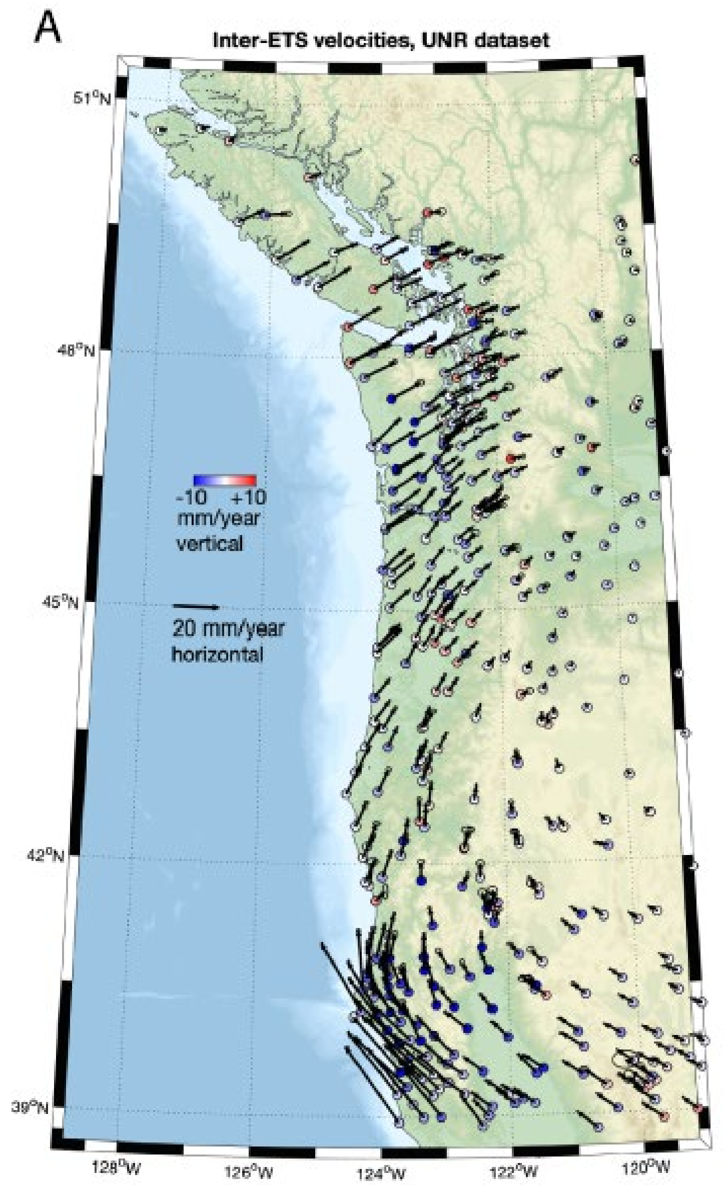

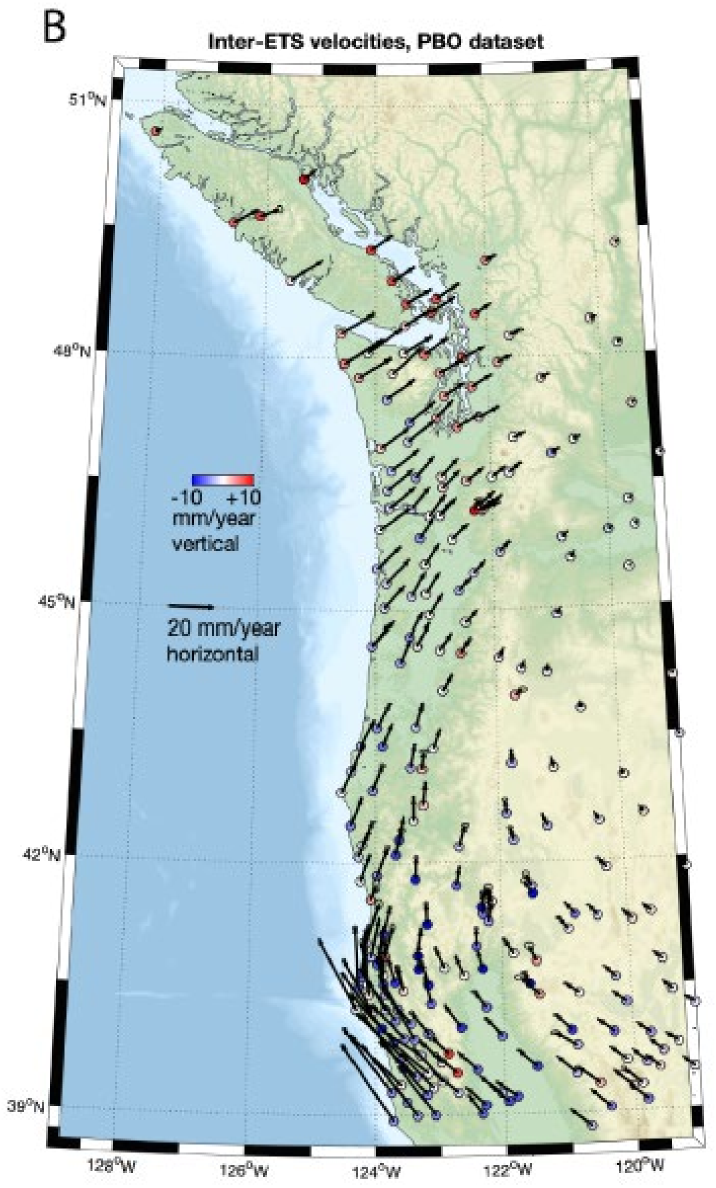

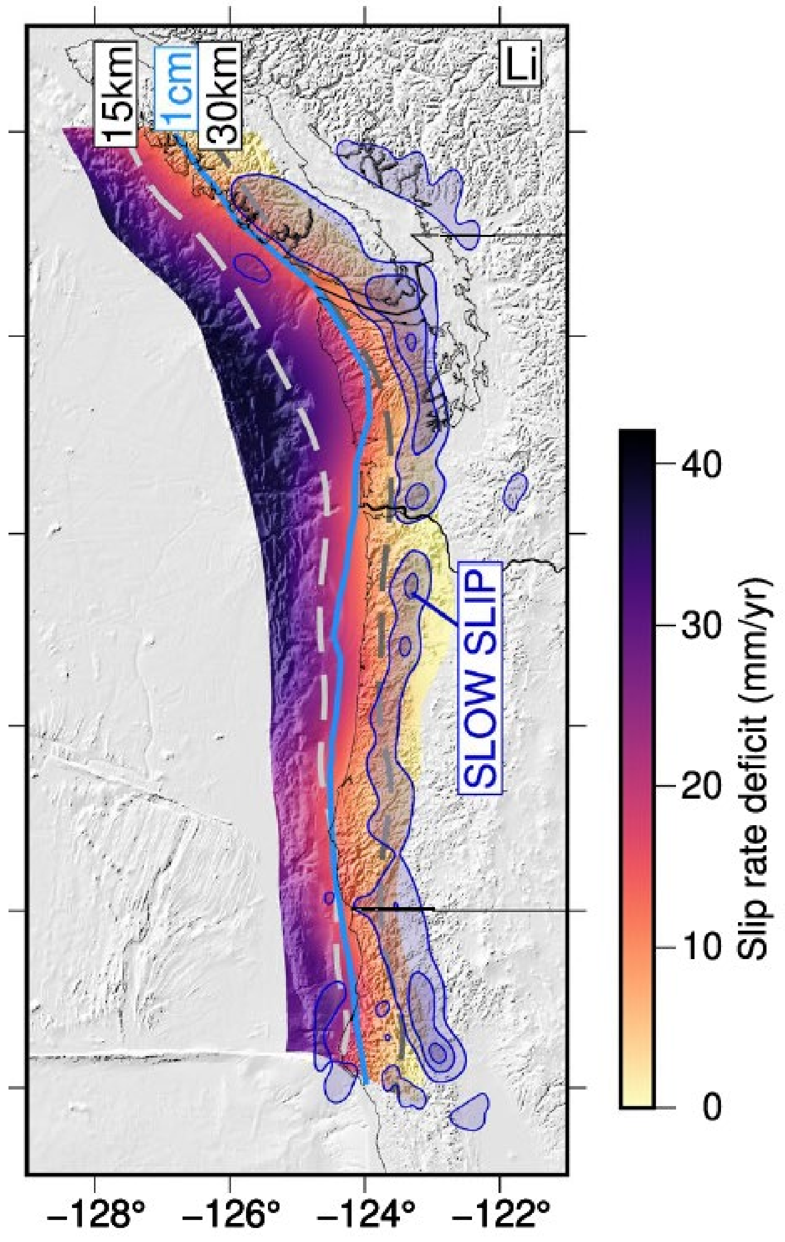

Cascadia slip deficit accumulation rate vs. Model Predictions

Li et al., 2018, Melgar et al., 2022-Geodesy
McCory et al., 2012-Geometry of the interface
Van Keken et al., 2019- Thermal structure

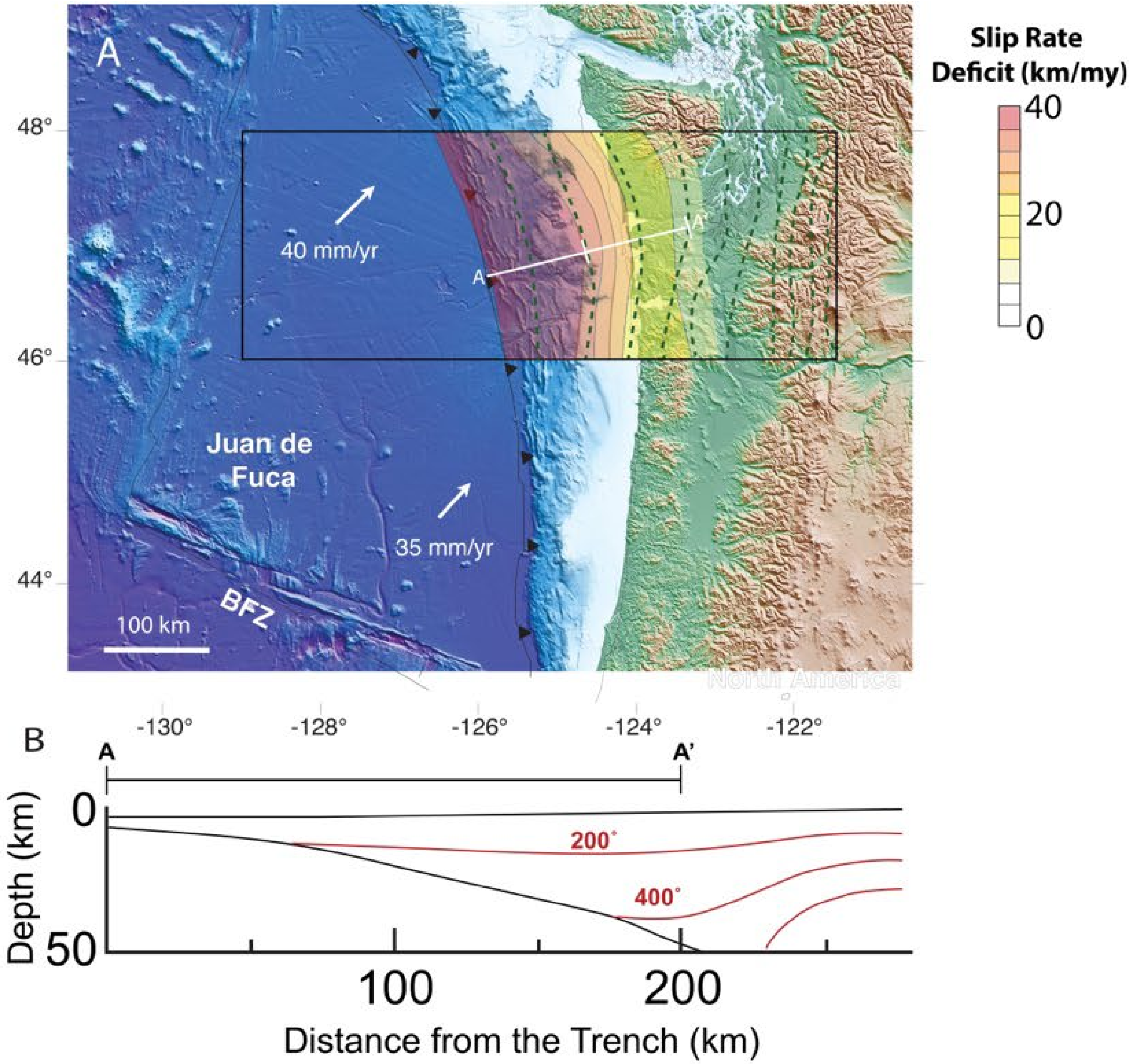

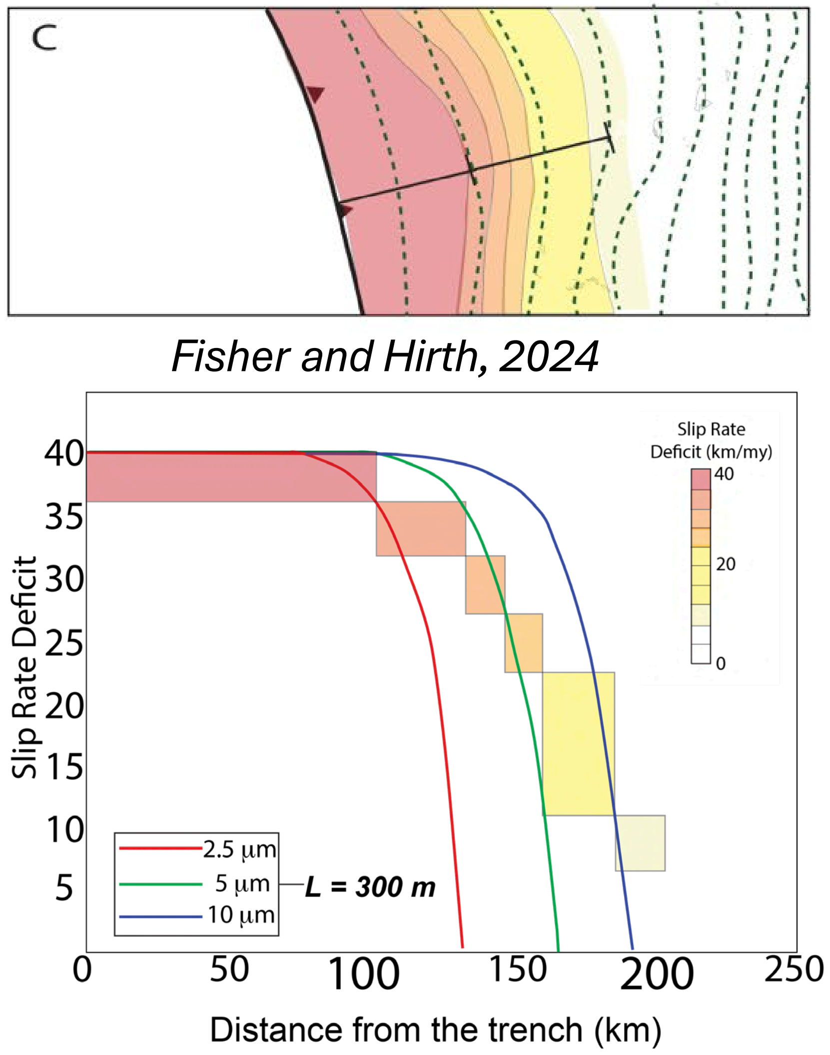

Fisher and Hirth, 2024

Role of mineral redistribution

- Mineral redistribution impacts both earthquake physics (by leading to variations in strength), and fluid flow (by generating variations in crack porosity, permeability, and fluid pressure).
- What are the feedbacks in the system and how do they modulate seismic and fluid flow behavior (i.e., observables)

Eq failure and healing

MEFISTO, the Mineralization, Earthquake, and Fluid-flow Integrated SimulaTOr

Fisher et al., 2019

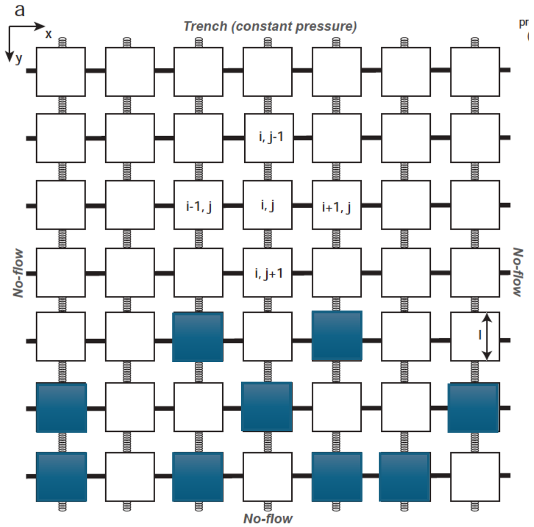

Plan View

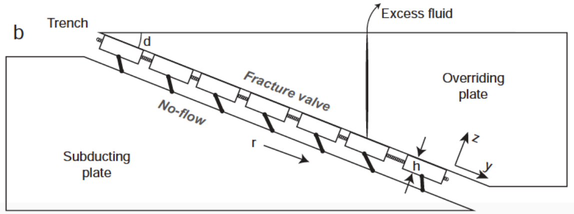

Cross sectional view

20 ˚

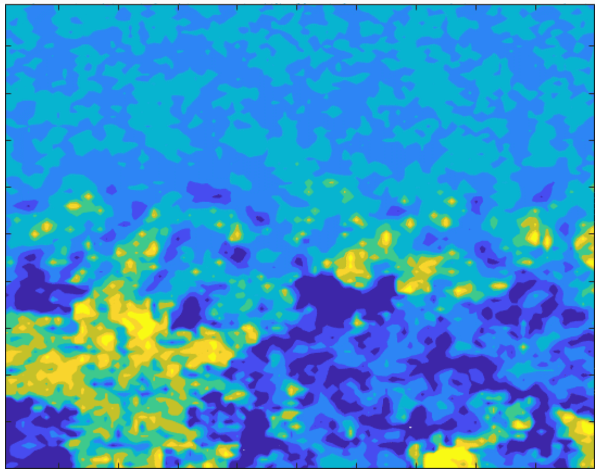

250 ˚

+ Pressure Solution

$$\dot{\varepsilon} = AC\sigma/d^3 \exp\left(-Q/RT\right)$$

+ Fluid Flow

Hooker and Fisher, 2021

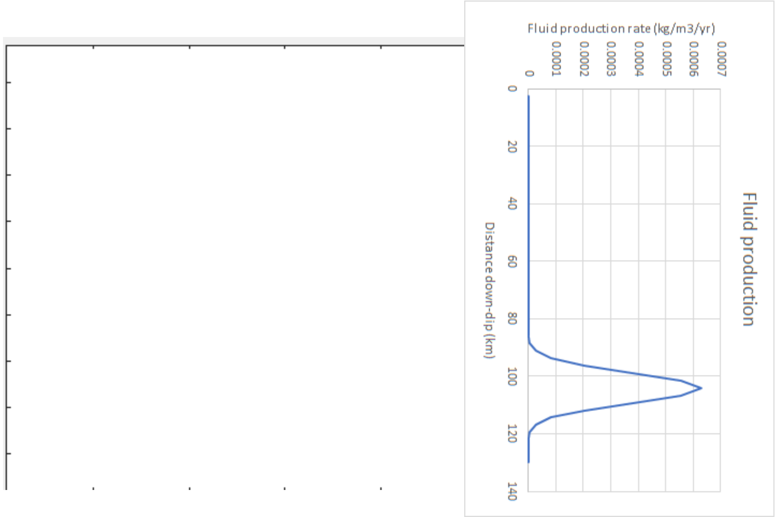

Zhuo et al., 2023

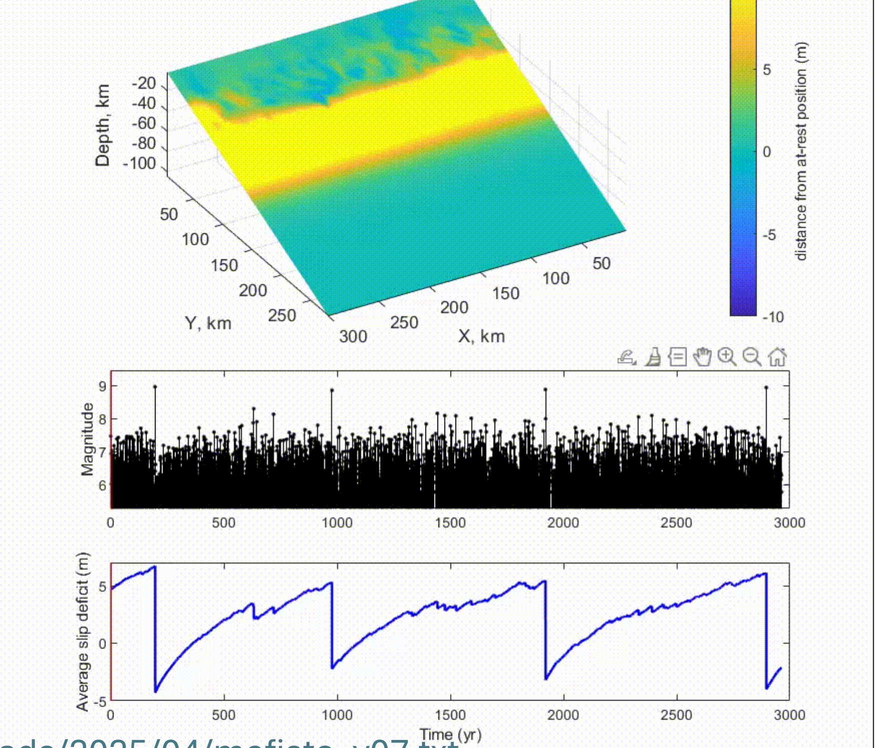

https://www.mefisto.org/wp-content/uploads/2025/04/mefisto_v07.txt

Slow Eqs near downdip limit-Cell 20

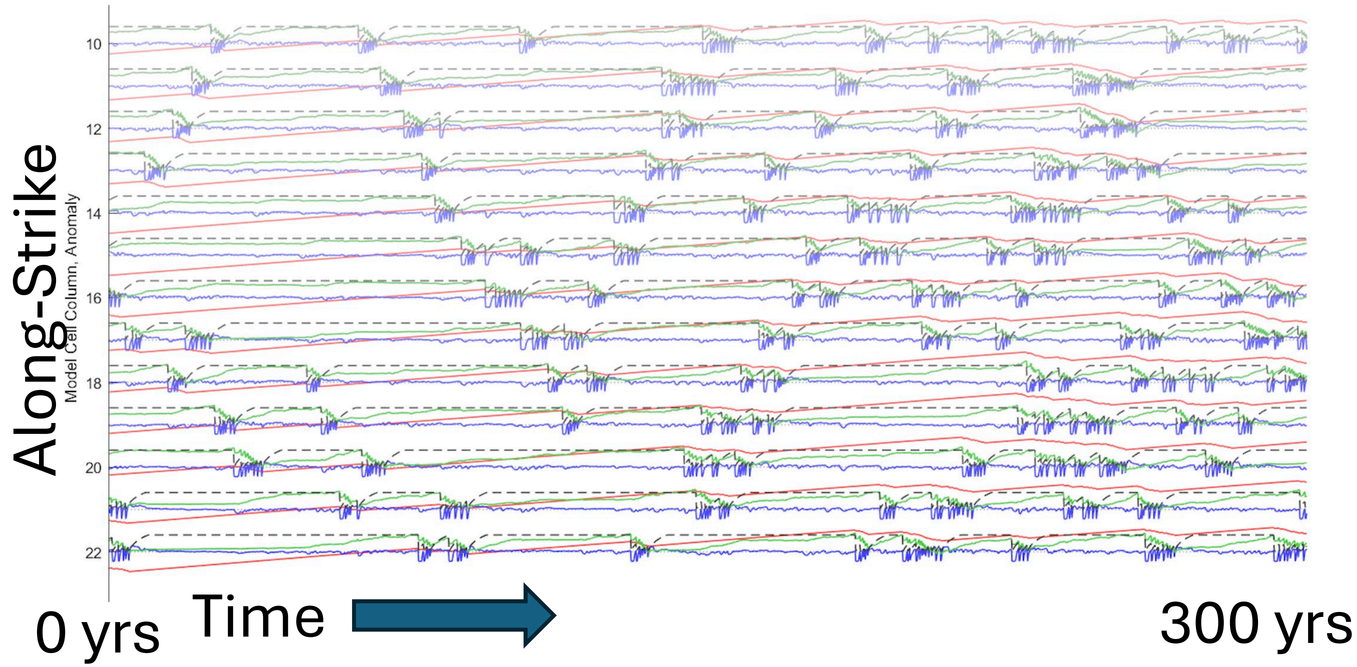

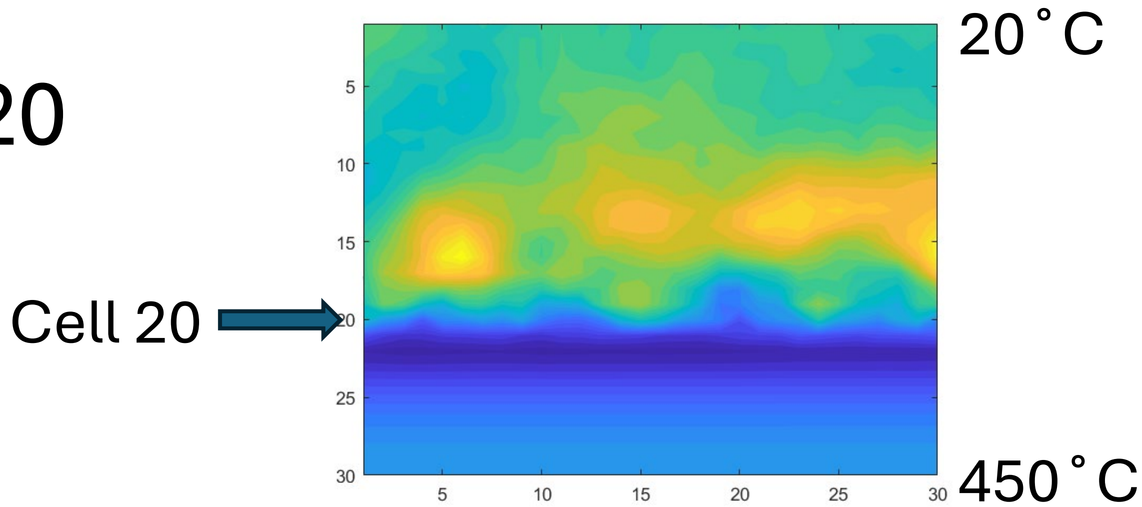

Slip Deficit

Fluid Pressure

Viscous flow rate/Plate rate

Asperity level

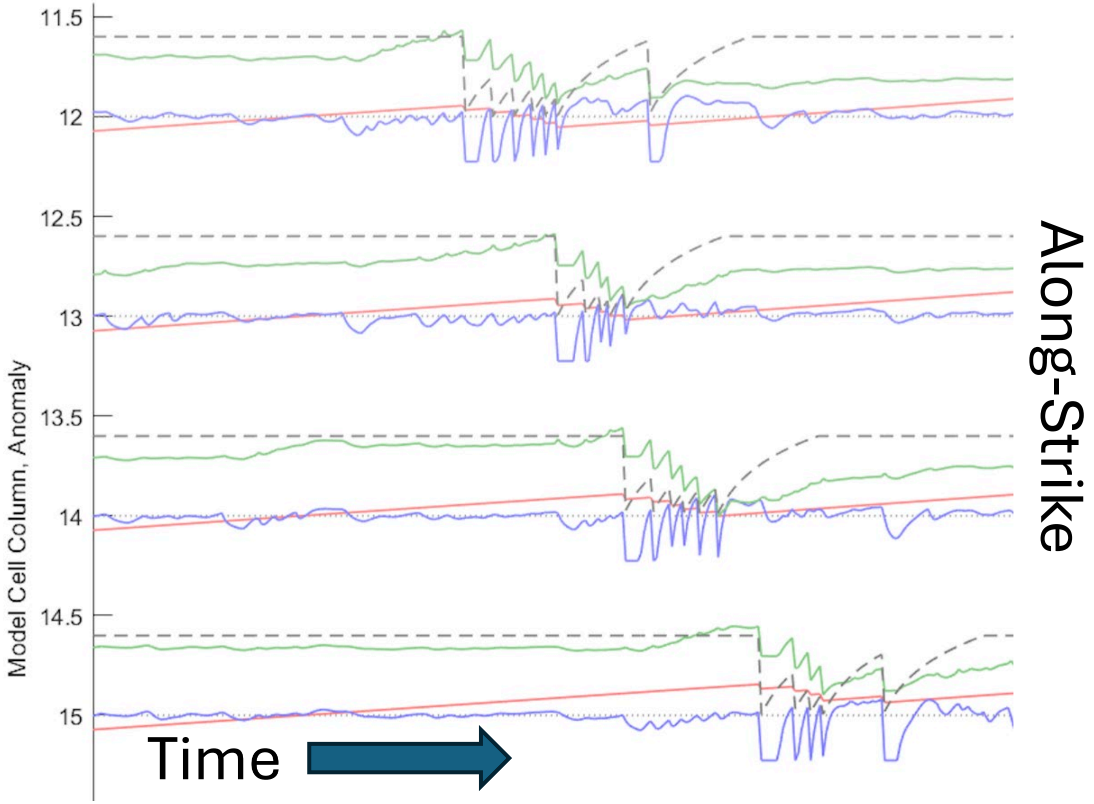

Quartz precipitation related to Advection

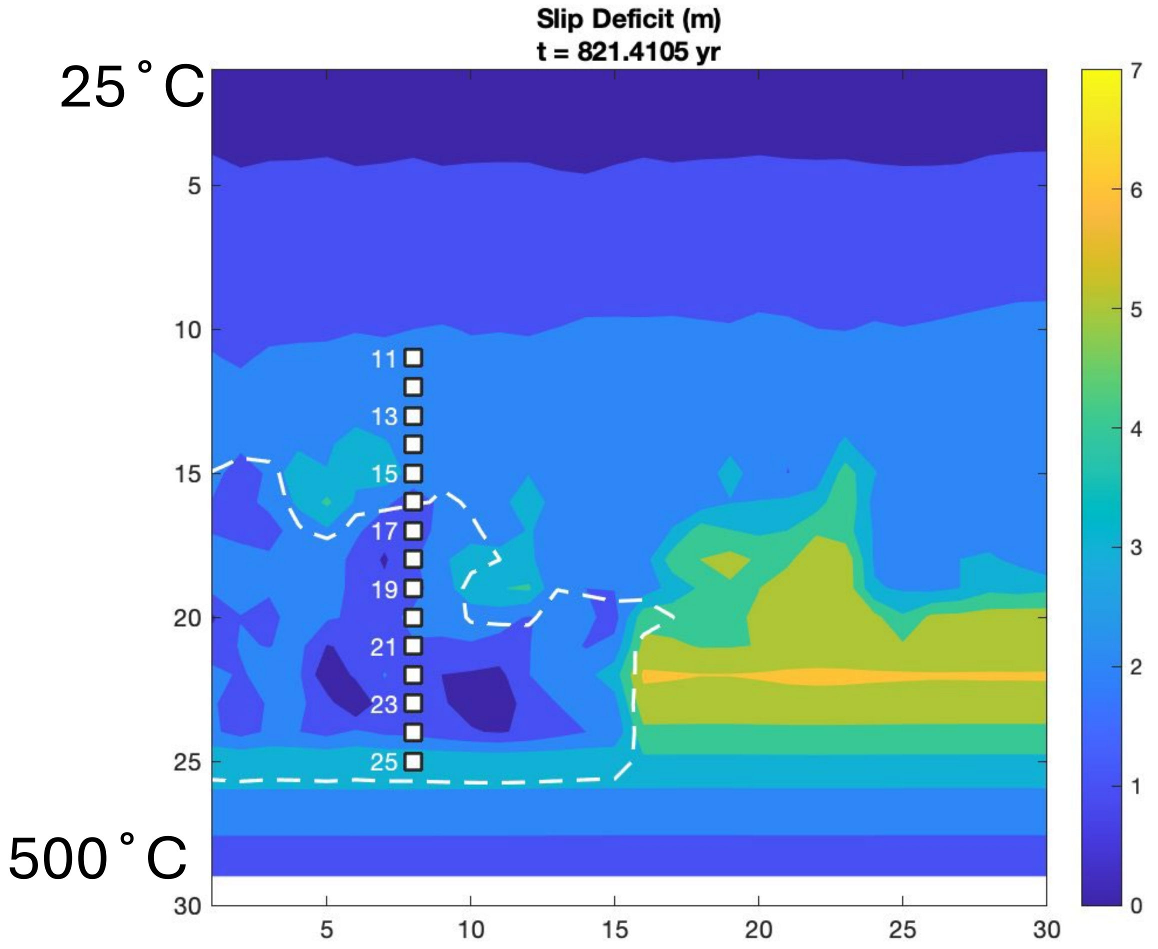

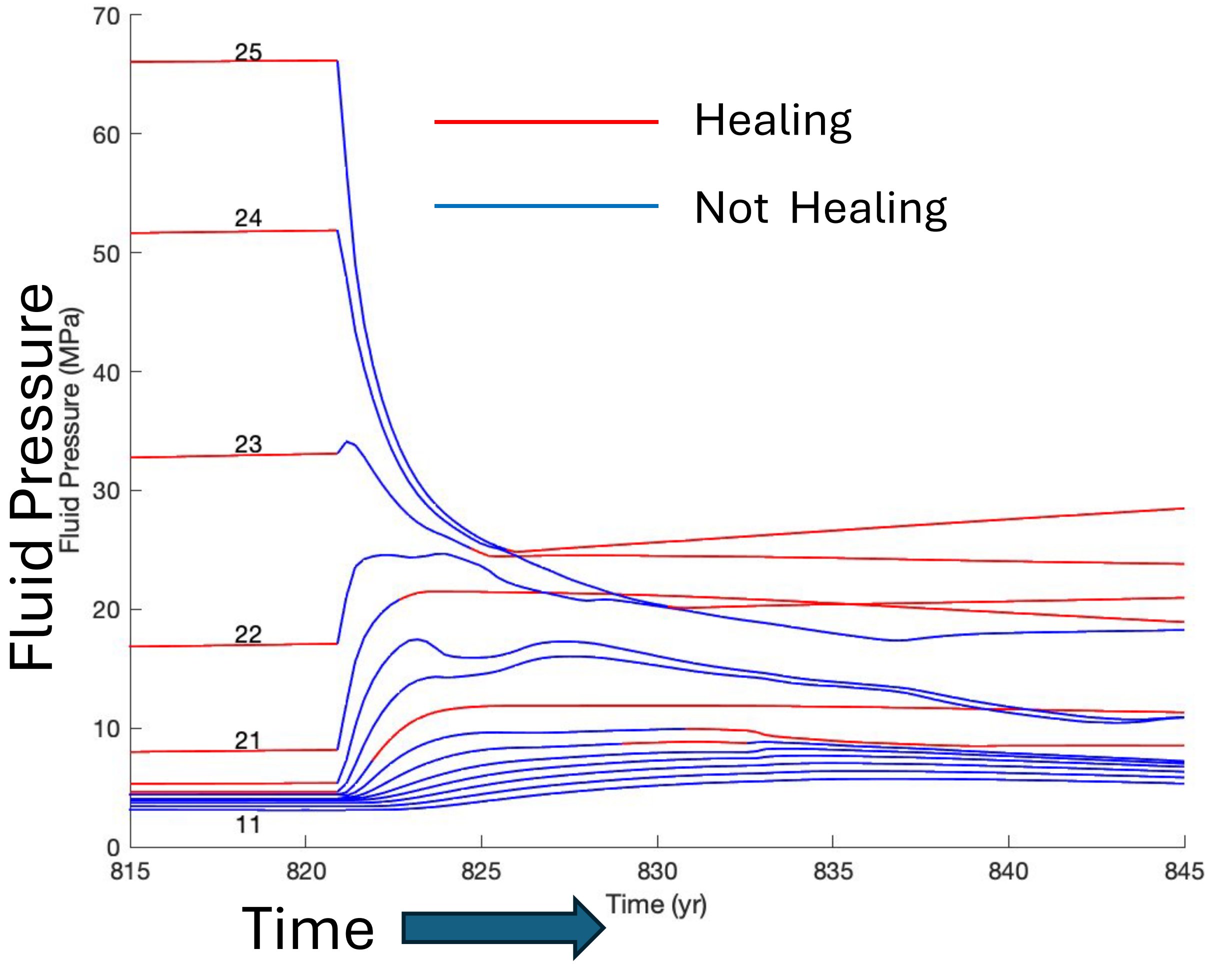

Quartz precipitation related to Advection

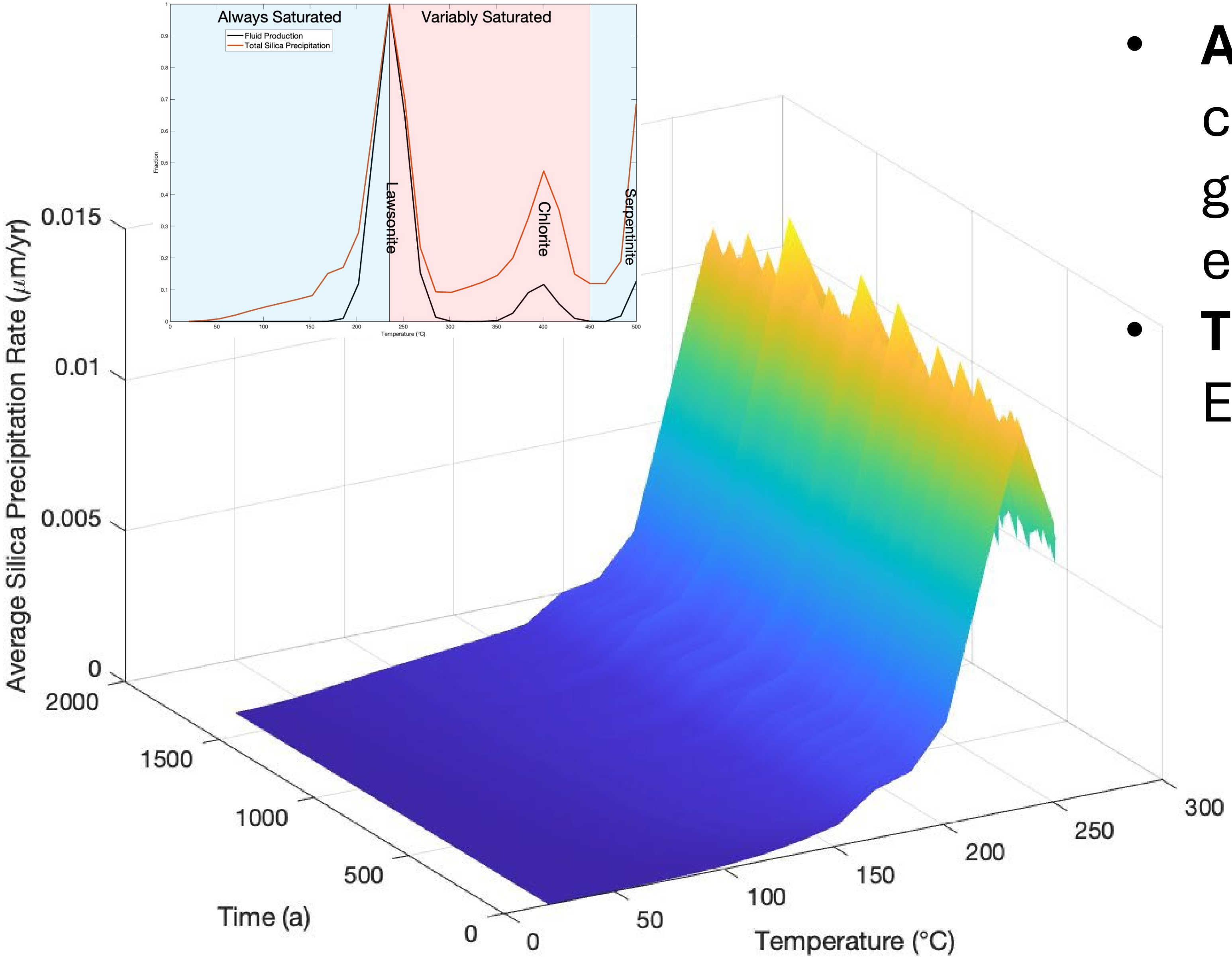

- **Ambient flow** down a chemical potential gradient of decreasing equilibrium solubility
- **Transients** related to Earthquakes

Take home: observed vein density along the interface are primarily a record of local diffusive transport

Conclusions

- Pressure solution is prevalent along the foot wall of the subduction interface and results in tectonic compaction and sealing of cracks.
- A flow law for pressure solution allows for extrapolation of strain rate downdip along the interface and across margins with different geometries and thermal structures, with tapering of slip deficit down to a temperature where ductile mechanisms can accommodate plate motions
- A numerical model shows that 3 factors-- 1) an earthquake simulator with temperature-dependent healing, 2) a fluid flow system, and 3) viscous interseismic deformation-- conspire to produce a range of slip behaviors observed along active margins.